Central European Journal of Geography and Sustainable Development
ISSN 2668-4322, ISSN-L 2668-4322

2025, Volume 7, Issue 1, Pages: 37-62
https://doi.org/10.51865/CEJGSD.2025.7.1.3

Non-rainy cloud cover dynamics and their influence on temperature variability in Chefchaouen, Western Rif, Morocco

Ayoub Al Mashoudi*

University of Abdelmalek Essaâdi, Faculty of Letters and Human Sciences, Department of Geography, Tetouan, Morocco;
ayoub.almashoudi@etu.uae.ac.ma

Received: 29 January 2025; Revised: 20 May 2025; Accepted: 26 May 2025; Published online: 17 June 2025

ABSTRACT: Non-precipitating cloud cover plays a significant role in modulating surface temperature by altering solar radiation and longwave heat retention. However, its thermal impacts remain underexplored in Mediterranean mountainous regions. This study investigates the influence of non-precipitating cloud cover on daily and seasonal temperature variability in Chefchaouen, Western Rif, Morocco, over a six-year period (2015–2020). The research classifies non-precipitating cloudy weather into three categories: (1) stable atmospheric conditions, (2) unstable atmospheric conditions, and (3) conditions at the periphery of frontal systems. High-resolution meteorological data, MODIS and NOAA satellite imagery, and synoptic weather maps were employed to analyze cloud-atmosphere interactions. Results reveal that stable cloud cover reduces the diurnal temperature range (DTR) by mitigating daytime heating and enhancing nocturnal warming. In contrast, unstable clouds increase thermal variability due to dynamic atmospheric processes. Seasonal effects were most pronounced in summer and winter, with notable moderation of temperature extremes. The findings highlight the role of synoptic-scale atmospheric structures, including sea-level pressure systems and 500 hPa geopotential height configurations, in shaping temperature variability under non-precipitating cloudy conditions. This study provides critical insights into Mediterranean climate dynamics and emphasizes the importance of integrating cloud-related processes into regional climate models to enhance temperature forecasting accuracy.

KEYWORDS: non-precipitating cloud cover, temperature variability, mediterranean climate, Chefchaouen, synoptic circulation patterns

TO CITE THIS ARTICLE: Al Mashoudi, A. (2025). Non-rainy cloud cover dynamics and their influence on temperature variability in Chefchaouen, Western Rif, Morocco. *Central European Journal of Geography and Sustainable Development*, *7*(1), 37–62. https://doi.org/10.51865/CEJGSD.2025.7.1.3

1. INTRODUCTION

Chefchaouen, located in the Western Rif Mountains of Morocco, is a distinctive climatic region shaped by its dual influence from the Atlantic Ocean and the Mediterranean Sea. Its unique geographical position, combined with the region's rugged mountainous topography, creates a highly sensitive environment to atmospheric circulation patterns, such as the North Atlantic Oscillation (NAO) and the Azores High (Lionello, 2006; Mashoudi et al., 2024; Trigo & Viterbo, 2003). While the Mediterranean climate is generally characterized by hot, dry summers and mild, wet winters, the Western Rif demonstrates complex climatic behavior driven by interactions between large-scale synoptic systems and localized microclimatic factors (Lennard & Hegerl, 2015; Newton et al., 2014). However, the specific role of non-rainy cloudy weather in shaping temperature patterns remains largely underexplored, particularly in mountainous regions.

* Corresponding author: ayoub.almashoudi@etu.uae.ac.ma; Tel.: +212-87430803

Cloud cover is widely recognized as a critical regulator of the Earth's energy balance, with dual impacts on surface temperatures. It reduces incoming solar radiation during the day and enhances longwave radiation retention at night, thus influencing the diurnal temperature range (DTR) (Zhu et al., 2024). Studies have shown that cloud cover can reduce DTR by 25% to 50% compared to clear-sky days, primarily due to its ability to limit surface solar radiation during the day, while having minimal influence on nighttime temperatures. However, in high latitudes during winter, clouds can increase nighttime temperatures due to their greenhouse effects (Dai et al., 1999; Jiang et al., 2022). This dual role of clouds underscores their significant contribution to surface temperature regulation and their broader implications for climate dynamics. Furthermore, as the atmosphere warms, a shift from ice to liquid-phase clouds introduces reflective and long-lived feedbacks, which reduce the absorbed solar flux and provide negative radiative feedback. Nevertheless, climate models often underestimate these effects due to biases in cloud precipitation-ralated processes (Mülmenstädt et al., 2021). These dynamics emphasize the need for more precise observational studies to improve the accuracy of climate projections.

In mountainous regions like Chefchaouen, the effects of cloud cover on temperature variability are amplified by the interactions between atmospheric dynamics and topographical features (He et al., 2020). Stable cloudy conditions are often associated with reduced DTR due to atmospheric stabilization, whereas unstable cloudy conditions may induce greater thermal variability as a result of dynamic atmospheric processes (Dai et al., 1999; Doan et al., 2022). Despite these well-documented phenomena, limited research has systematically addressed the thermal impacts of non-rainy cloudy weather in Mediterranean mountainous contexts, leaving a significant knowledge gap regarding localized climate dynamics.

This study aims to address this gap by investigating the influence of non-rainy cloudy weather on daily and seasonal temperature variability in Chefchaouen over a six-year period (2015–2020). This timeframe was carefully selected based on the availability of high-resolution meteorological data, ensuring the reliability and robustness of the analysis. The comprehensive datasets collected during this period allow for an in-depth exploration of cloud-atmosphere interactions in Chefchaouen, a region that exemplifies the complex interplay between Mediterranean climatic influences and mountainous topographical dynamics.

Chefchaouen was specifically chosen as the study site due to its climatic complexity and the intricate interactions between synoptic-scale weather systems, localized microclimatic conditions, and mountainous topography. Previous studies have highlighted the region's significant spatial variability in land surface temperature (LST), driven by its heterogeneous topography and land cover, as well as its vulnerability to natural hazards like landslides, which are influenced by geological and climatic factors (El Kharim et al., 2021; Raissouni et al., 2013). These characteristics make Chefchaouen an ideal location for investigating the thermal impacts of non-rainy cloudy weather in a Mediterranean mountainous context.

To analyze the thermal impacts of cloudy weather, this study adopts a well-established classification of non-rainy cloudy weather, originally developed by Vigneau (1985), El Baye (1990) and Arraji (1995). This classification categorizes non-rainy cloudy weather into three distinct types: (1) stable atmospheric conditions, (2) unstable atmospheric conditions, and (3) conditions occurring at the periphery of frontal systems. Building on this framework, the present study examines how cloud cover interacts with atmospheric circulations to regulate surface temperatures in this climatically and geographically sensitive region.Variations in cloud cover significantly influence surface air temperature (SAT) by modulating radiation processes: during the day, clouds block incoming solar radiation, causing cooling, while at night, they trap outgoing longwave radiation, resulting in warming. This diurnal asymmetry in cloud effects has been identified as a key amplifier of surface warming in the context of increasing greenhouse gas concentrations (Luo et al., 2024). Moreover, as the atmosphere warms, the shift from ice to liquid-phase clouds introduces reflective and long-lived feedbacks, although uncertainties remain in climate models due to biases in cloud precipitation-related processes (Mülmenstädt et al., 2021). By focusing exclusively on non-rainy periods, this study seeks to isolate these subtle yet critical dynamics within the unique climatic context of Chefchaouen.

The study adopts an integrated methodology, combining high-resolution meteorological data with synoptic weather maps to identify the atmospheric configurations associated with each cloudy weather type. It tests the hypothesis that non-rainy cloudy weather significantly moderates temperature extremes, particularly in summer and winter, when thermal variability is most pronounced. Preliminary findings

suggest that cloudy weather plays a pivotal role in dampening temperature extremes and stabilizing thermal conditions, highlighting its relevance in regional climate modulation.

This research not only contributes to the scientific understanding of Mediterranean climate variability but also has practical applications for improving weather forecasting and guiding climate adaptation strategies. By shedding light on cloud-atmosphere interactions, the findings can inform critical sectors such as agriculture, water management, and urban planning, emphasizing the need for incorporating these dynamics into regional climate models for sensitive and understudied regions like Chefchaouen.

2. LITERATURE REVIEW

The relationship between cloud cover and surface temperature has been widely explored across different climatic zones, particularly in the context of global and regional climate change. Early foundational work by Lamb (1972) and later by Jones et al. (1993) developed weather type classifications that continue to underpin synoptic climatology today. These frameworks have been essential for identifying patterns of atmospheric circulation and their influence on weather dynamics, including temperature variability.

In the Moroccan and broader Mediterranean context, Vigneau (1985) offered significant methodological tools for interpreting synoptic conditions, which were later adapted by El Baye (1990, 1992) and Arraji (1995) to fit local climatic specificities. These classifications remain central to climatological studies in North Africa. However, their application has often been limited to identifying macro-scale weather types, with less emphasis on the thermal implications of non-precipitating cloudy conditions—especially in mountainous regions.

Several international studies have documented the thermal modulation effect of cloudiness, emphasizing its dual role in limiting solar radiation during the day and enhancing longwave radiation at night (Dai et al., 1999; Groisman et al., 2000). These findings are consistent across regions characterized by complex topography and transitional climates (Jiang et al., 2022). In Mediterranean settings, Pyrgou et al. (2019) and Katavoutas et al. (2023) highlighted the role of cloud cover in mitigating summer temperature extremes. Xu et al. (2021), focusing on the Himalayas, demonstrated that increased cloudiness is associated with more stable thermal regimes, a dynamic that may also apply to high-altitude areas in North Africa.

Despite these contributions, limited empirical work has been dedicated to understanding how distinct categories of non-rainy cloudy weather impact temperature variability on a seasonal and daily basis. The present study revisits and applies established classifications (Lamb, 1972; Vigneau, 1985; El Baye, 1990) in a focused regional context—Chefchaouen, northern Morocco—to examine how selected cloud types (fairly stable, quite unstable, and marginal frontal) correlate with temperature variation. Rather than proposing a novel framework, this analysis seeks to deepen the understanding of existing schemes by integrating long-term meteorological data with synoptic interpretation.

This approach aligns with the broader literature calling for more nuanced, location-specific climate diagnostics, particularly in regions marked by orographic and maritime influences. By contributing to this analytical strand, the study supports the growing effort to localize climate impact assessments, providing a reference for regional planning, environmental monitoring, and policy adaptation under evolving climatic conditions.

3. RESEARCH METHODS

3.1. Study area

Chefchaouen, located in the western Rif region of Morocco at 35.1715° N and 5.2697° W (Figure 1), enjoys a distinctive climatic profile shaped by its position between the Atlantic Ocean and the Mediterranean Sea. This unique location, combined with the complex topography of the Rif Mountains—featuring peaks like Jbel Lakrâa (2,159 meters) and Jbel Tissouka (2,122 meters)—creates diverse microclimates. The interaction of steep slopes and deep valleys with atmospheric circulation patterns significantly impacts temperature and precipitation (Hssaisoune et al. 2022; Todaro et al. 2022).

The region's orographic features enhance precipitation at higher elevations through the orographic lifting of moist air masses, while the rain shadow effect causes drier conditions on the leeward side of the

mountains (El Alaoui El Fels et al., 2022). These topographical and meteorological interactions generate sharp contrasts in thermal and precipitation regimes over short distances (Camici et al., 2018). Furthermore, the moderating influence of the Atlantic Ocean and the Mediterranean Sea helps stabilize the climate, with the Canary Current along the Atlantic coast dampening daytime heat intensity and maintaining higher humidity levels during summer (Mills, 2024; Semedo, 2018).

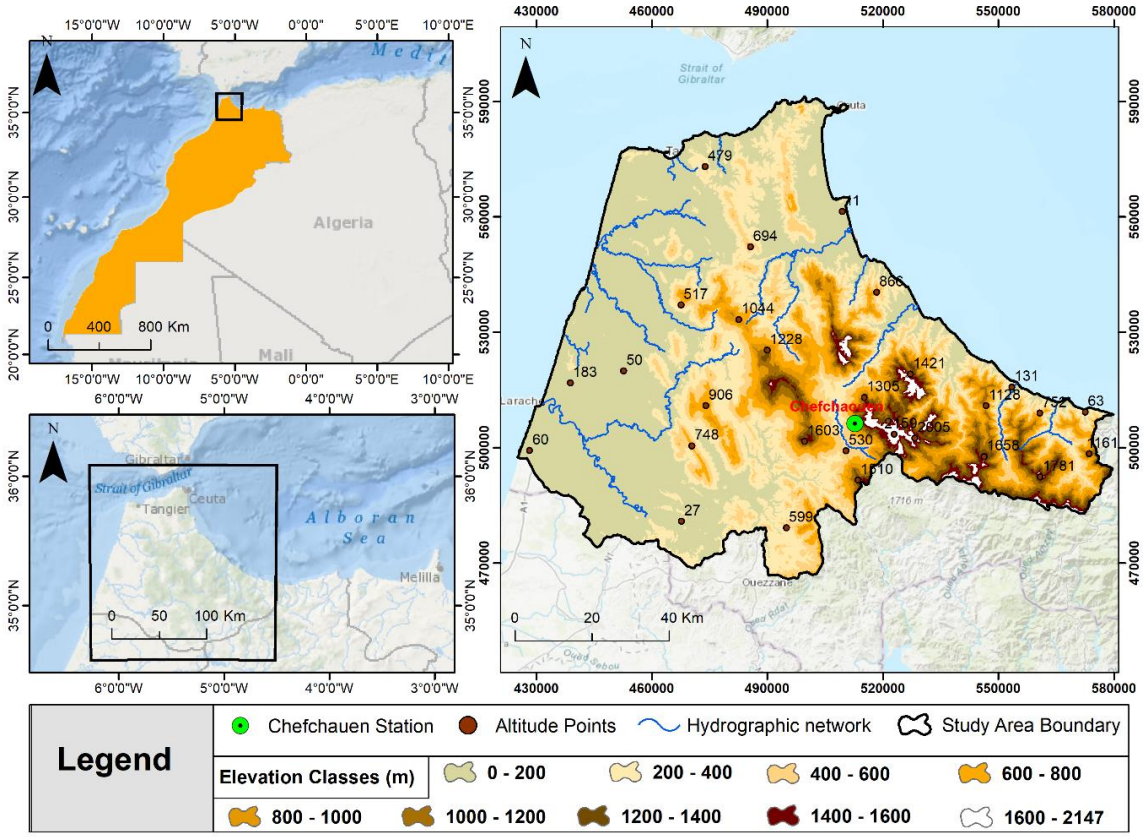

Figure 1. Localization of the study area.
Source: Created by the author (2025).

Over the 1995–2020 period, Chefchaouen's climate exhibited strong seasonal variability. Average monthly temperatures ranged from 4.2°C (January) to 34.3°C (August), reflecting cold, wet winters and hot, dry summers. Rainfall was highly concentrated between November and March, with a monthly peak of 199.9 mm in December, while the summer months, especially July and August, remained virtually dry (less thn 3 mm/month). Annual precipitation averaged around 930 mm, but showed sharp interannual fluctuations, from a minimum of 372.3 mm (2015) to a maximum of 2,422.8 mm (1996). This climatic regime reinforces the region's sensitivity to hydro-climatic extremes and highlights the importance of understanding seasonal and interannual variability in any environmental or hydrological assessment of the area.

This interplay between maritime and topographical influences establishes Chefchaouen as a region of significant climatic heterogeneity. Detailed investigations into these dynamics are essential for understanding the area's environmental characteristics, including localized wind systems, temperature inversions, and variable precipitation patterns (Dezfuli et al., 2015). Such studies provide valuable insights into the region's hydrological processes and ecosystem dynamics (Bonino et al., 2019; Fang et al., 2010).

3.2. Data

This study utilized a dataset provided by the National Meteorological Office of Morocco (DMN), which included daily temperature records and weather conditions from the Chefchaouen meteorological station (coordinates: 35°10'21" N, 5°18'47" W, elevation: 287 meters). Covering the period from 2015 to 2020,

the dataset comprised daily average, maximum, and minimum temperatures, as well as total daily precipitation and cloud cover observations. All data were subjected to rigorous quality control and validation procedures, including cross-referencing with nearby stations and detecting statistical anomaly detection.

To enhance the analysis of cloud cover and atmospheric conditions, satellite imagery from MODIS (Moderate Resolution Imaging Spectroradiometer) and NOAA (National Oceanic and Atmospheric Administration) was incorporated. These platforms offer moderate spatial resolution but high temporal frequency, enabling detailed monitoring of cloud formations, dynamics, and atmospheric structures. By integrating satellite data with ground-based measurements, the study provided a comprehensive framework for cloud classification, as supported by Zhang et al. (2011)

Aerological datasets were also utilized, covering both surface conditions (mean sea level pressure, MSLP) and upper-atmosphere dynamics (500 hPa geopotential height). This multi-level approach allowed for a nuanced understanding of atmospheric behavior. Weather maps from global models, including the Global Forecast System (GFS) and the European Centre for Medium-Range Weather Forecasts (ECMWF), were analyzed to investigate atmospheric patterns. Synoptic charts obtained from the Wetterzentrale platform, which hosts data from Deutscher Wetterdienst (DWD) and NOAA-GFS, provided additional insights into regional and global weather patterns dating back to 1979.

To reconcile the observation periods across these diverse datasets, ground-based, satellite, and aerological, the study adopted a synchronous, case-based selection protocol focused exclusively on the 2015–2020 period. Cloudy weather cases without recorded precipitation were first identified using MODIS and NOAA imagery, and then cross-referenced with local rainfall data from the Chefchaouen station. Only days fulfilling both criteria, visual cloud presence and zero precipitation, were retained. For those same dates, 500 hPa and MSLP fields were extracted from GFS and ECMWF archives to characterize the prevailing synoptic conditions. This strategy ensured full temporal alignment across all datasets and enabled the derivation of consistent weather pattern typologies.

Nevertheless, the use of daily temperature data has inherent limitations. While useful for long-term trend analysis, such data often fail to capture short-term fluctuations and extreme weather events. For instance, daily temperature measurements, typically recorded as maximum and minimum values, cannot adequately reflect rapid changes caused by localized phenomena like thunderstorms or sudden wind shifts (Zhang et al., 2011). Similarly, extreme events such as heatwaves, which are often most intense in the afternoon, are averaged out, thereby underestimating their severity (Perkins et al., 2012). In mountainous regions like the Rif, variations in altitude create significant microclimatic differences within short distances, complicating the use of daily averages for precise climate assessments (Fowler et al., 2007).

3.3. Classification method

3.3.1. Basis and approach

Various classification systems have been developed to study atmospheric patterns and their influence on regional weather. For example, the Grosswetterlagen system (James, 2007) focuses on long-term sea-level pressure patterns, while the Lamb Weather Types (Jones et al., 1993; Lamb, 1972) classify weather based on wind direction and pressure systems. These systems illustrate the diversity of approaches available for categorizing atmospheric dynamics, highlighting the adaptability required for different climatic and geographic contexts. In this study, we adopted a modified version of the classification methodology developed by Vigneau (1985), El Baye (1990) and El Baye (1992), and Arraji (1995), tailored to the subtropical characteristics of Chefchaouen.

To classify cloudy weather patterns, this study utilized Mean Sea Level Pressure (MSLP) data in conjunction with high-resolution satellite imagery from MODIS and NOAA. "Cloudy weather with fairly stable atmospheric conditions," classified with 1-4 octas of cloud cover, reflects weak disturbances or localized convective processes, often with minimal dynamic changes (Appendix I). "Cloudy weather with quite unstable atmospheric conditions" (4-8 octas) typically corresponds to upper-level disturbances or approaching frontal systems, resulting in significant cloud cover (Appendix II). Lastly, "Cloudy weather occurring at the margins of frontal systems" refers to complex synoptic conditions where nearby frontal boundaries influence local weather without dominating it (Hoskins & Karoly, 1981)(Appendix III).

To enhance accuracy, satellite data were integrated with synoptic weather charts to analyze transient phenomena and upper-level disturbances influencing cloud patterns. By combining MSLP data with satellite imagery, this approach captured surface-level dynamics and their connections with upper-atmospheric circulations (Kalisch & Macke, 2008; Philipp, 2009). This combination strengthened the robustness of the classification process

3.3.2. Encoding and categorization

To facilitate detailed daily analysis, atmospheric circulation patterns were classified based on MSLP and upper-level circulation at 500 hPa. These levels are particularly relevant for identifying daily variability due to their role in shaping weather dynamics (Dilling et al., 2017; Hufty, 2005; Liu et al., 2014). Each weather scenario was encoded using a two-letter code system: the first letter indicates the general characteristics of the air masses, while the second letter describes the sky's regional state (Appendix IV). Additional codes represented other non-precipitating weather types (see Table 1 for details).

Table 1. Frequency percentage of non-precipitating weather and its corresponding code.

Cloudy Non-Rainy Weather Types	Frequency (%)	code
Cloudy weather with fairly stable atmospheric conditions	17.5	(1)
Cloudy weather with quite unstable atmospheric conditions	16.0	(2)
Cloudy weather occurring at the margins of the frontal systems	6.5	(3)

Source: Classification adapted from Vigneau (1985) and El Baye (1990); frequency analysis by the author.

Frequencies of weather types were calculated by analyzing occurrences within the six-year dataset, allowing for detailed categorization. For example, code 3 represents weather influenced by nearby frontal systems but not dominated by them, often resulting in variable cloud cover without significant precipitation (Table 1).

3.3.3. Analysis and visualization

The study analyzed the relationship between MSLP and 500 hPa circulations to identify patterns driving non-rainy cloudy weather. Sea-level pressure systems (e.g., cyclones, anticyclones) influence wind patterns and precipitation, while 500 hPa patterns (e.g., Rossby waves) shape regional variability (Hoskins & Karoly, 1981; Peña et al., 2011). By associating recurring atmospheric structures with weather types, average temperatures were calculated for each type over the six-year period. This allowed the study to link atmospheric dynamics to temperature variability.

Figures included in Appendix IV illustrate the methodological framework adopted in this study, detailing the classification of atmospheric circulation patterns and their influence on temperature variability in the Western Rif region. These figures provide a comprehensive representation of high and low-pressure system configurations, with colored lines indicating the relative positions of isobaric structures. Additionally, the two figures presented above will be incorporated into the appendices to further clarify the synoptic conditions affecting the study area. A legend is provided within each figure to facilitate interpretation, ensuring a precise understanding of the atmospheric mechanisms shaping weather patterns in this complex mountainous region.

The study excluded weather types not directly relevant to its objectives (e.g., low stratiform clouds independent of disturbed systems) to maintain focus. Seasonal temperature trends for each weather type were represented visually, with months color-coded (red for summer, blue for winter, etc.), providing an intuitive understanding of the data.

4. RESULTS

4.1. Cloudy weather with fairly stable atmospheric conditions (1)

The "Cloudy weather with fairly stable atmospheric conditions (1)" classification occurred 387 times over the study period, representing 17.5% of all recorded cases (Table 1). This weather pattern demonstrates notable seasonal variations, with the highest frequency observed during the summer months (38.5%), followed by winter (22.4%), autumn (19.8%), and spring (19.3%) (Figure 2).

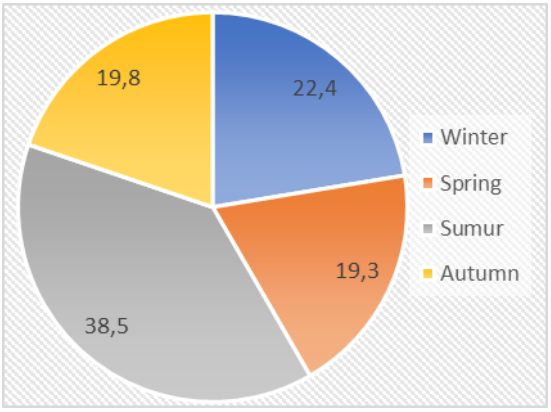

Figure 2. Seasonal Distribution of Cloudy weather with fairly stable atmospheric conditions (1) Occurrences (%).
Source: Created by the author based on seasonally categorized meteorological data.

Building on these seasonal variations, further analysis of sea-level pressure (SLP) configurations provides deeper insights into the mechanisms driving stable, cloudy weather conditions. These configurations highlight the specific atmospheric patterns responsible for the observed variations across seasons.

The seasonal data on sea-level pressure (SLP) configurations reveal significant variation in cloudy weather occurrences under stable atmospheric conditions (1) across different seasons (Figure 3).

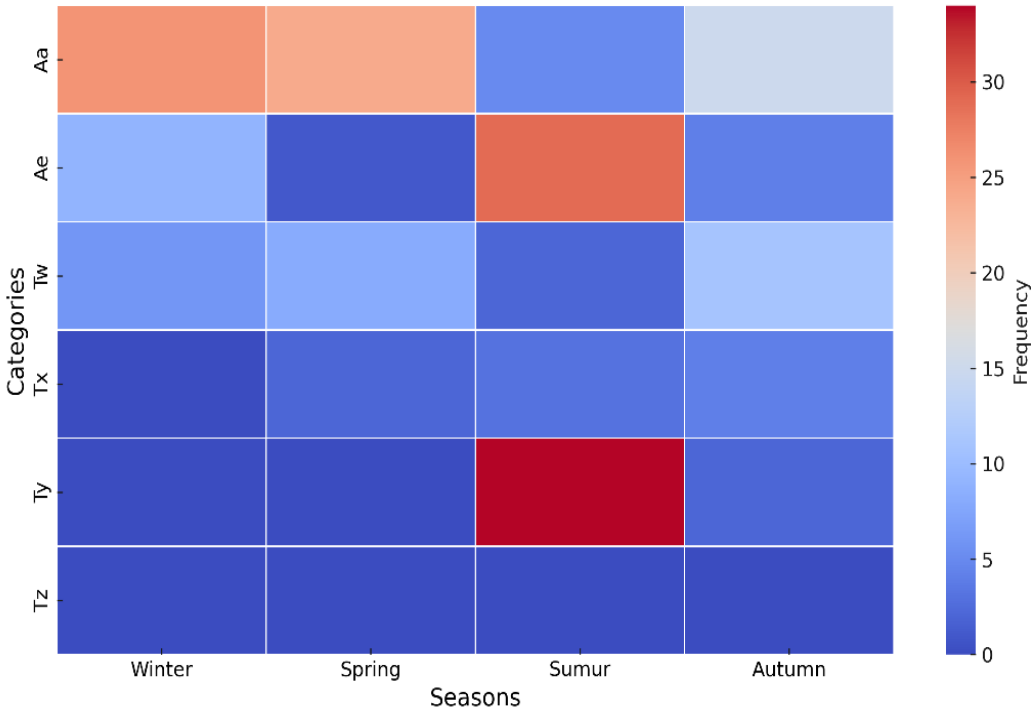

Figure 3. Seasonal distribution of sea-level pressure (SLP) configurations for Cloudy weather with fairly stable atmospheric conditions (1) conditions.
Source: Visualization created by the author based on categorized meteorological data (Chefchaouen Station).

Summer exhibits the highest frequency of these configurations, with Tz being the most prominent, reflecting the influence of stable, high-pressure systems during this period. Despite the general atmospheric stability during (1) conditions, the presence of sufficient relative humidity in the mid-troposphere contributes to the formation of light, intermittent clouds (Groisman et al., 2000; Kolendowicz et al., 2021), particularly during transitional phases such as the Tz configuration in summer. In contrast, winter is marked by the presence of Aa, representing the high pressure centered over the Atlantic Ocean,

contributing to stable weather conditions but at a lower frequency compared to summer (Figure 3). Other configurations, such as Tw and Ae, are more evenly distributed during the transitional seasons of spring and autumn, where shifting atmospheric patterns play a critical role in shaping relatively stable cloudy weather. These seasonal variations underscore the importance of different atmospheric configurations in influencing weather stability across the year.

The seasonal data on 500 hPa pressure configurations reveal significant variation in cloudy weather occurrences under stable atmospheric conditions (1) across different seasons (Figure 4). Summer shows the highest frequency, with Sg occurring 18 times and Cd appearing 13 times, reflecting the influence of stable upper-level systems during this period. In contrast, winter is marked by the presence of Ng, which occurs 14 times, associated with northerly currents contributing to stable weather, though less frequently than in summer. Other configurations, such as Vc in autumn with 10 occurrences and Cc in spring with 7 occurrences, are more evenly distributed during the transitional seasons, where shifting atmospheric patterns shape relatively stable cloudy weather. These seasonal variations underscore the importance of upper-atmospheric configurations in influencing weather stability throughout the year.

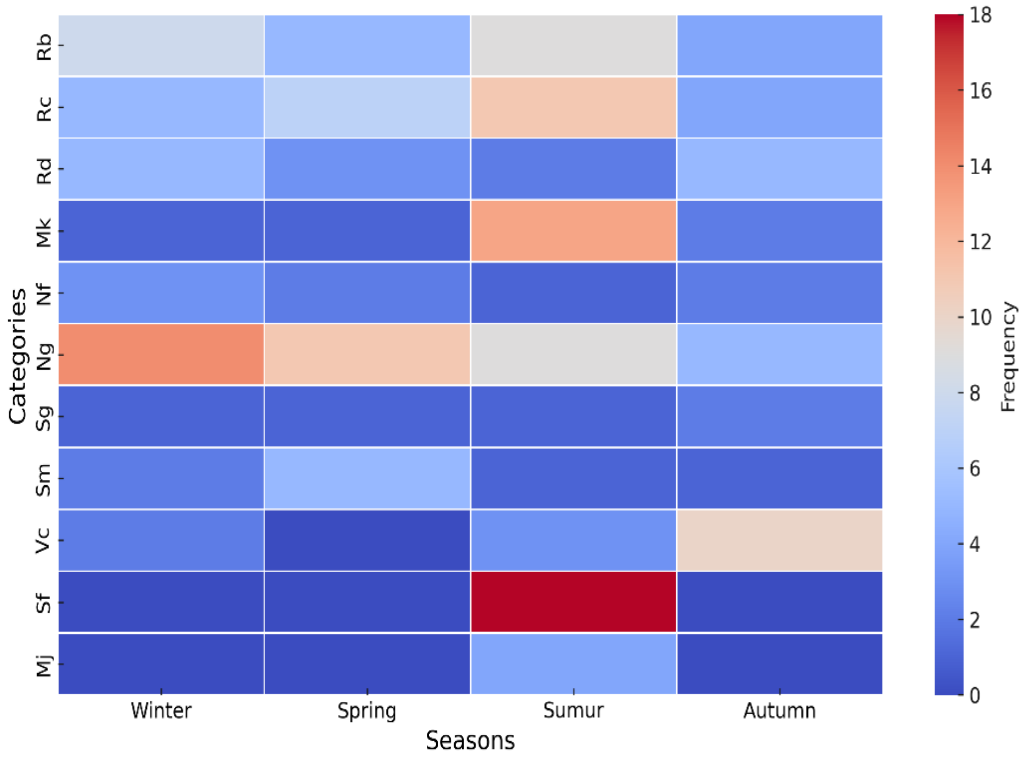

Figure 4. Seasonal distribution of sea-level pressure (500 hPa) configurations for Cloudy weather with fairly stable atmospheric conditions (1) conditions.
Source: Visualization created by the author based on categorized meteorological data (Chefchaouen Station).

The distinction between the roles of surface-level pressure (SLP) and the 500 hPa level in shaping weather patterns is fundamental in meteorology. Surface-level pressure systems, such as high-pressure formations (e.g., Aa and Ae), primarily modulate local temperature variations and wind patterns by regulating the advection and movement of air masses.

At the 500 hPa level, the dynamics of the atmosphere function on a broader scale, governing large-scale circulation patterns. Ridges and troughs at this altitude play a pivotal role in either maintaining atmospheric stability or inducing changes. While these upper-level systems do not directly influence surface temperatures, they set the stage for surface-level pressure systems to exert their influence by creating more stable or unstable atmospheric conditions. Understanding the processes at 500 hPa is essential for interpreting the synoptic-scale mechanisms behind cloud formation, air mass movements, and the broader weather patterns that manifest at the surface (Jabbar & Hassan, 2023; Li et al., 2018; Loikith et al., 2019).

The interaction between upper- and lower-atmospheric systems is what ultimately shapes observable weather conditions. For instance, ridges at 500 hPa influence the persistence of high-pressure systems at the surface, such as Aa and Ae, which in turn regulate local temperature fluctuations and cloud formation. Figure 5 highlights this correlation by illustrating how specific temperature variations align with different atmospheric configurations, showcasing the interdependence between upper-level patterns and surface-level weather dynamics.

This temperature classification, ranging from 28.3°C to 19°C, encompasses approximately 46.5% of the overall cases (Figure 5). Notably, high temperatures are predominantly associated with ridges (Teng & Branstator, 2017) in various branches, including Ca, Cb, and Cd. This relationship is crucial for understanding heatwaves and climate anomalies (Li et al., 2018; Loikith & Kalashnikov, 2023). Additionally, a "no gradient configuration" or "uniform field" (Mk) contributes to these elevated temperatures by making weather conditions homogeneous. This leads to a stable weather pattern without significant changes or movements. Such uniform atmospheric conditions often contribute to partly cloudy skies, especially cirrus clouds. This setup, characterized by minimal variations in pressure and temperature, allows for stable conditions that can lead to the formation of scattered clouds. These conditions are typical in high-pressure systems, where limited vertical air movement results (Wang et al., 2020). At the surface level, these high temperatures correlate with transitional situations, specifically the barometric swamp (Tw), followed by scenarios where the pressure equals 1015 hPa (Tz).

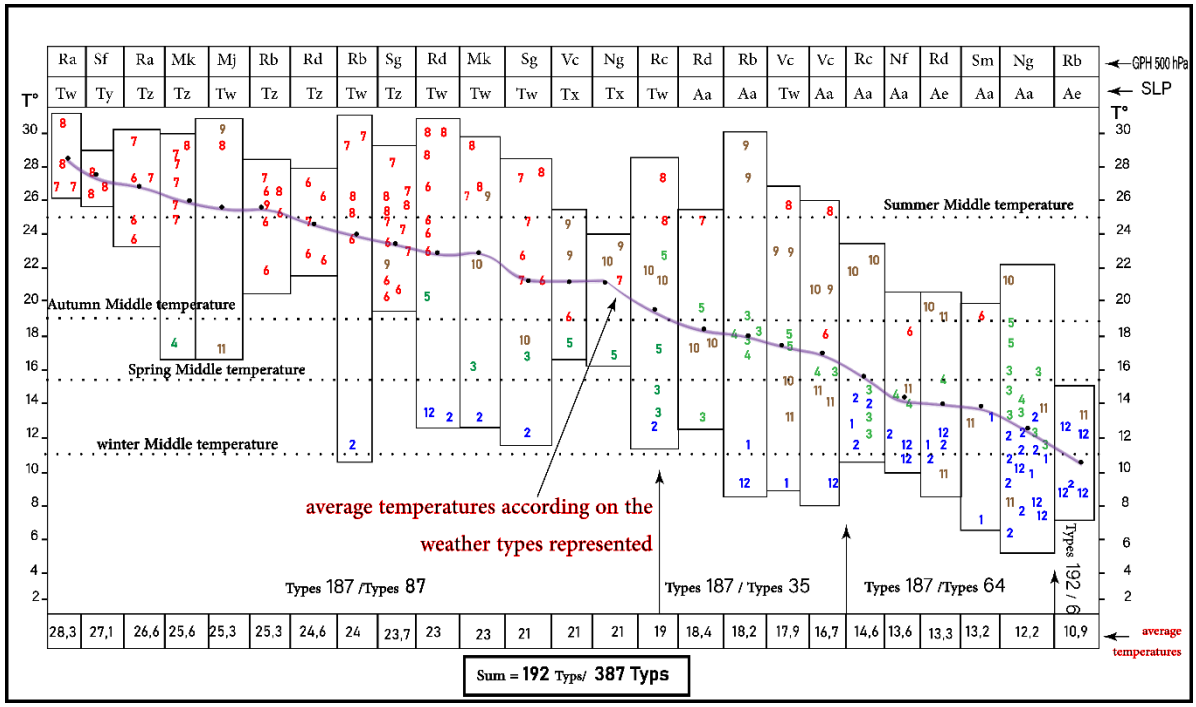

Figure 5. Impact of cloudy weather under relatively stable atmospheric conditions on average temperatures at Chefchaouen Station, based on the analysis of atmospheric structures at 500 hPa and sea level. This figure represents approximately 50% of all recorded weather cases of type (1). The highest average temperature observed was 28.3 °C, associated with the Ca-Tw atmospheric structure, while the lowest average temperature, 10.9 °C, was linked to the Cb-Ae structure. These conditions were most frequently recorded during the summer season, as shown by the predominance of red-shaded months corresponding to summer.

Source: Created by the author based on processed meteorological data.

The classification between 19°C and 16°C comprises approximately 18.8% of the cases. This classification is particularly indicative of the transitional seasons, namely spring and fall, where notable ridges exert significant influence on most circulations at the 500 hPa level, including Cc, Cd, Cb, and Vc. During these two seasons, the atmospheric circulation patterns at the 500 hPa level can lead to substantial shifts in air mass movements, resulting in warmer or cooler than average conditions depending on the prevailing ridge or trough patterns (Gillett et al., 2006; Grimm et al., 2000). This is evident in the

noticeable decline in average daily temperatures within this classification, where temperatures shift from 19°C in the Cc configuration to 16°C in the Vc configuration (Figure 5).

The temperature continues to drop in the classification between 16°C and 12°C. This classification represents 33.3% of the total cases depicted in Figure 15. Predominantly observed during the winter months (December, January, and February), it extends to certain spring and fall months, contributing to a decline in the average temperature within this classification. Observations at the 500 hPa level show a significant presence of formations from the North Current (Ng and Nf). This indicates a shift in atmospheric conditions, moving from a state dominated by ridges to one potentially governed by troughs. This transition results in the introduction of northern or northwesterly air masses, leading to the development of scattered clouds. At the surface level, prevailing situations involve the Azores High (Aa) and the European High (Ae).

The classification of cases with temperatures lower than 10°C is the least frequent, representing 3.1% of the total cases depicted, primarily observed in December and January. At the 500 hPa level, well-defined ridges (Cb) dominate, indicating that ridges do not always result in higher temperatures (Figure 5). In this scenario, temperatures dropped to approximately 8.5°C, with high pressure at the surface (Ae) over Europe contributing to cold, stable conditions. This suggests that even in the presence of ridges, the movement and positioning of high-pressure systems play a critical role in determining temperature and cloud formation patterns.

4.2. Cloudy weather with quite unstable atmospheric conditions (2)

The classification of "Cloudy weather with quite unstable atmospheric conditions (2)" occurred 349 times throughout the study, representing 16% of the total recorded cases (Table 1) (Figure 6). This weather pattern displays considerable seasonal variation, with its highest frequency in autumn (27.9%), followed by summer (27.3%) and winter (25%), as illustrated in Figure 9. The lowest frequency was recorded in spring, at 19.8% (Figure 6).

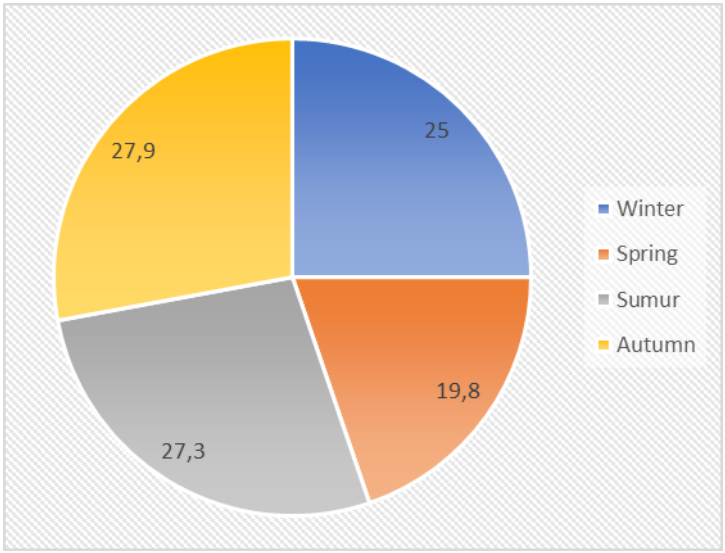

Figure 6. Seasonal Distribution of Cloudy weather with quite unstable atmospheric conditions (2).
Source: Created by the author based on seasonally categorized meteorological data.

The atmospheric configurations at sea level pressure (SLP), depicted in Figure 7, highlight distinct seasonal patterns. For example, the "Aa" structure dominates both winter and spring, whereas the "Tz" structure prevails during summer, correlating with more unstable conditions. This suggests that such patterns have a direct influence on the variability and frequency of cloudy and unstable conditions across seasons.

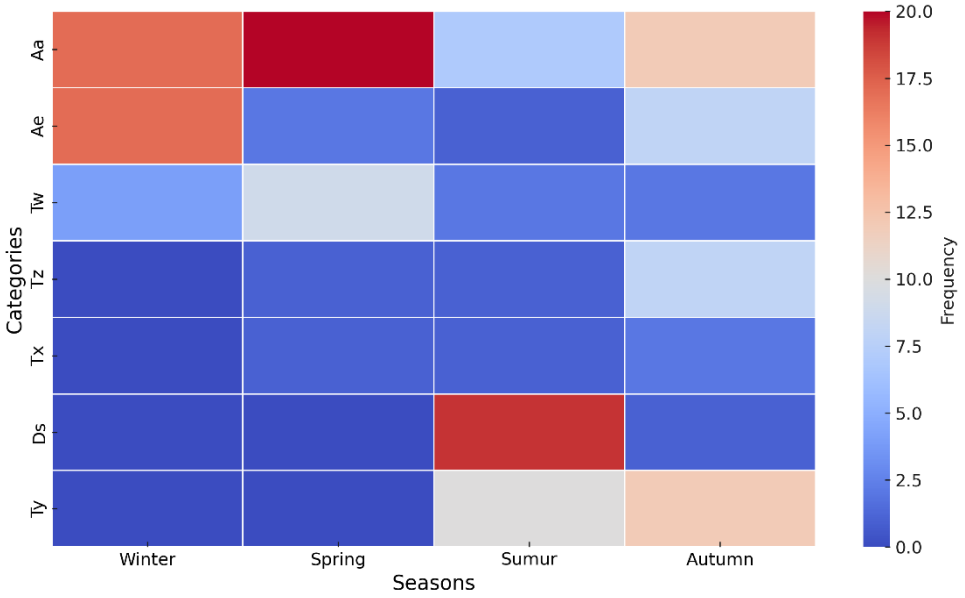

Figure 7. Seasonal distribution of sea-level pressure (SLP) configurations for Cloudy weather with quite unstable atmospheric conditions (2) conditions.
Source: Visualization created by the author based on categorized meteorological data (Chefchaouen Station).

At the 500 hPa level (Figure 8), seasonal variability is further illustrated. The "Cb" structure, representative of Ridge activity, plays a vital role in winter, especially over Western Europe and North Africa. These high-pressure systems block westerly flows, creating prolonged periods of dry and stable weather, notably over the Mediterranean. However, this blocking effect can result in extreme events, such as cold spells, due to the interaction between Ridge and cold air masses from the north (Kautz et al., 2022; Rojas et al., 2013). The "Sg" structure becomes predominant in summer, associated with increased occurrences of this weather pattern. It transports warm, moist air from subtropical regions toward North Africa and southwestern Europe, enhancing humidity and cloud formation without necessarily causing precipitation (Akinsanola & Zhou, 2020; Gatzen, 2020; Yang et al., 2023). The interaction between SLP and 500 hPa structures is essential in driving the seasonal dynamics of this weather type.

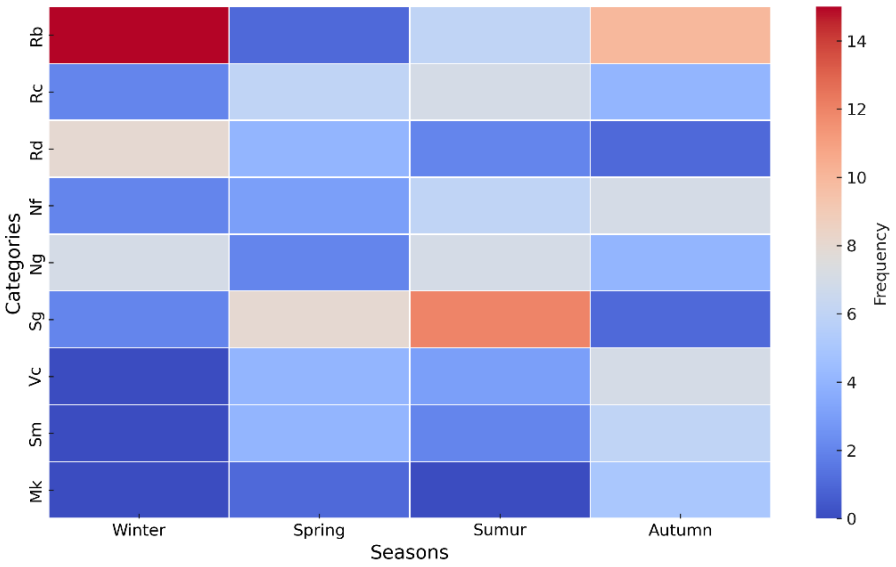

Figure 8. Seasonal distribution of sea-level pressure (500 hPa) configurations for Cloudy weather with quite unstable atmospheric conditions (2) conditions.
Source: Visualization created by the author based on categorized meteorological data (Chefchaouen Station).

Figure 9 illustrates approximately half of these occurrences, with the violet dashed line representing the average temperature, highlighting the thermal variations associated with various atmospheric structures. Notably, there is a significant temperature decline after stabilizing at structures (Mk-Tz), indicating a shift in the atmospheric system that directly affects temperatures. The temperature continues to decrease at a normal rate until the structure (Cc-Tw), where another temperature drop occurs.

The (2) weather condition occurred 349 times, accounting for 16% of all cases. Figure 9 illustrates approximately half of these occurrences, with the violet dashed line representing the average temperature. This line highlights the thermal variations associated with various atmospheric structures. Notably, there is a significant temperature decline after stabilizing at structures (Mk-Tz), indicating a shift in the atmospheric system that directly affects temperatures. The temperature continues to decrease at a normal rate until the structure (Cc-Tw), where another temperature drop occurs. This trend, shown in Figure 9, underscores the dynamic nature of atmospheric changes and their implications for weather patterns (Byrne & Schneider, 2018; Horton et al., 2015; Zappa, 2019).

Temperatures ranging from 29°C to 20°C make up 49.4% of all cases, with the summer months (June, July, and August) being the most represented in this range. Transitional phases are frequently observed at the surface level, particularly through Tz and Tw, with high-pressure conditions notably absent. At the 500 hPa level, ridge movements decline while valleys (Vc) increase, indicating weak polar descents halting over regions such as the Iberian Peninsula or Central Europe. Atmospheric changes often intensify near Morocco (García-Valero et al., 2012; Gonçalves et al., 2023; Pereira et al., 2021). Southern currents, like Sm and Sg, are indicative of imminent weather changes, characterized by dropping temperatures, increased cloud cover, and potential light to moderate winds (Ghassabi et al., 2022; Jabbar & Hassan, 2023; Loikith et al., 2019).

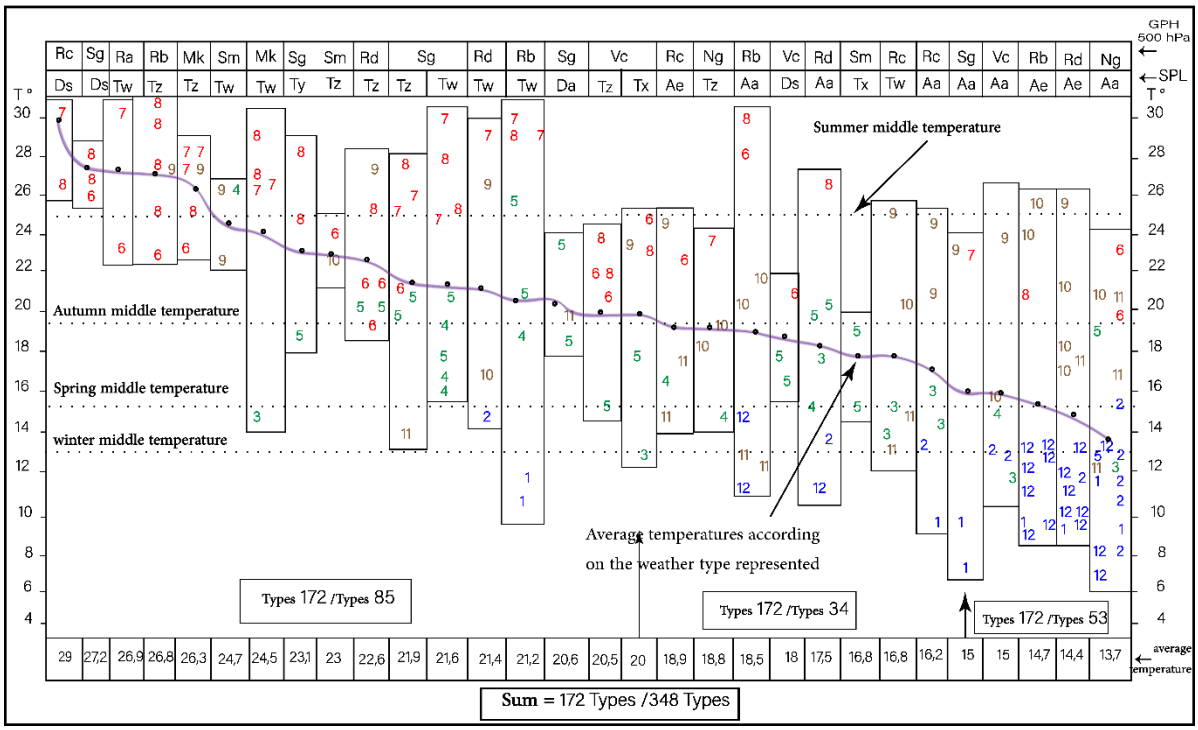

Figure 9. Impact of cloudy weather with notably unstable atmospheric conditions on average temperatures at Chefchaouen Station, based on the analysis of atmospheric patterns at 500 hPa and sea level. This figure represents approximately 50% of the weather cases categorized as type (2-1). Average temperatures exceeded 30 °C under several configurations, including (Ca-Tw), (Cb-Tz), (Sg-Tw), and (Cb-Aa), suggesting that upper-level ridges and transitional conditions at sea level significantly contribute to high-temperature events. Conversely, marked temperature drops were observed under configurations such as (Cb-Ae), (Cd-Ae), and (Ng-Aa), which occurred more frequently in winter. These patterns highlight the seasonal variability and thermal contrast of this weather type, where temperatures can range from over 30 °C to as low as 13.7 °C, characteristic of cloudy and highly unstable atmospheric situations.
Source: Created by the author based on processed meteorological data.

Temperatures between 19°C and 15°C constitute about 20% of all cases (Figure 9). These are mainly associated with Cb and Cc structures, correlating with recurring Aa and Ae states at the sea level. Such conditions create atmospheric consistency within the troposphere, often resulting in stable, cloudy skies, as vertical air movements are minimized (Lu et al., 2019). This phenomenon is particularly common during the winter months, where it recurs more frequently compared to other seasons., as supported by previous studies (Groisman et al., 2005; Kautz et al., 2022; Rojas et al., 2013; Sun et al., 2000). Cloud cover during these periods plays a key role in modulating temperature extremes by blocking solar radiation during the day and trapping heat at night, reducing the diurnal temperature range (Kay et al., 2016).

Finally, temperatures ranging between 15°C and 13.7°C account for 30.8% of cases. These conditions, specific to transitional seasons, show a noticeable and continuous temperature drop, with no stabilization across different atmospheric structures (2).

4.3. Cloudy weather occurring at the margins of the frontal systems (3)

In this study, the term "margin" is used in a geographical sense, as defined by (Keyser 1986; El Baye A 1990; Anand and Pal 2023). The weather condition 'Cloudy weather occurring at the margins of frontal systems (3)' was observed 143 times, constituting 6.5% of all recorded instances during the study period, with notable seasonal variation (Table 1). The highest occurrence was recorded in spring (38.2%), followed by winter (24.5%) and summer (23.5%), while autumn marks the lowest frequency at 13.7%, as shown in Figure 10. Cases (3) depicted in Figure 10 account for over 55% of the total occurrences. This weather condition occurs when a front passes near our study area from the west or north, where the area does not typically experience all the characteristics of the front, particularly precipitation. Instead, the sky is covered with high cumulus clouds, temperatures drop, and wind speeds increase (Beckert et al., 2023; Browning et al., 1982).

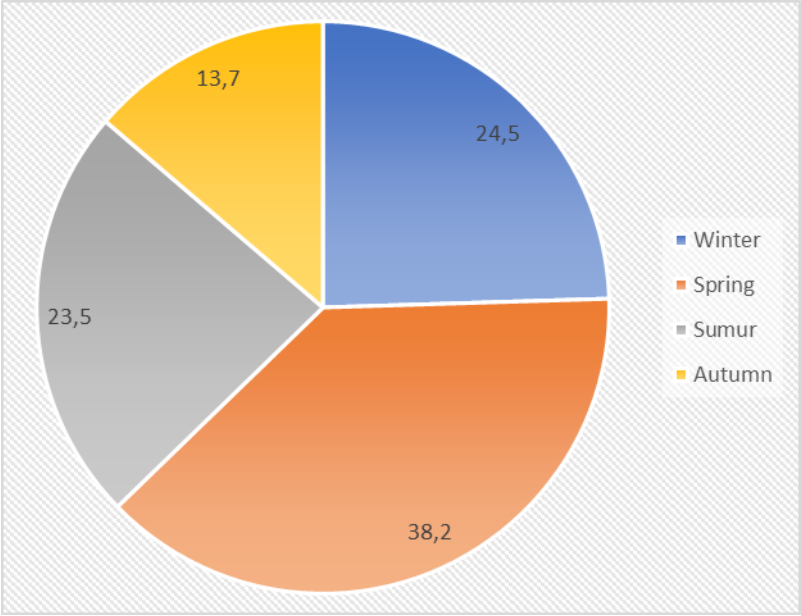

Figure 10. Seasonal Distribution of Cloudy weather occurring at the margins of the frontal systems (3). Source: Created by the author based on seasonally categorized meteorological data.

The atmospheric configurations at sea level pressure (SLP) reveal distinct seasonal variations, as shown in Figure 11. The "Aa" structure is particularly dominant in winter, with 13 occurrences, and remains significant in spring with 7 occurrences. In contrast, the "Tz" structure becomes most prominent during summer, registering 10 occurrences, reflecting more unstable conditions during this period. Additionally, other structures such as "Da" and "Tw" show moderate activity, especially during spring and summer. These patterns clearly illustrate how seasonal variability influences the frequency of cloudy and unstable weather conditions across different times of the year.

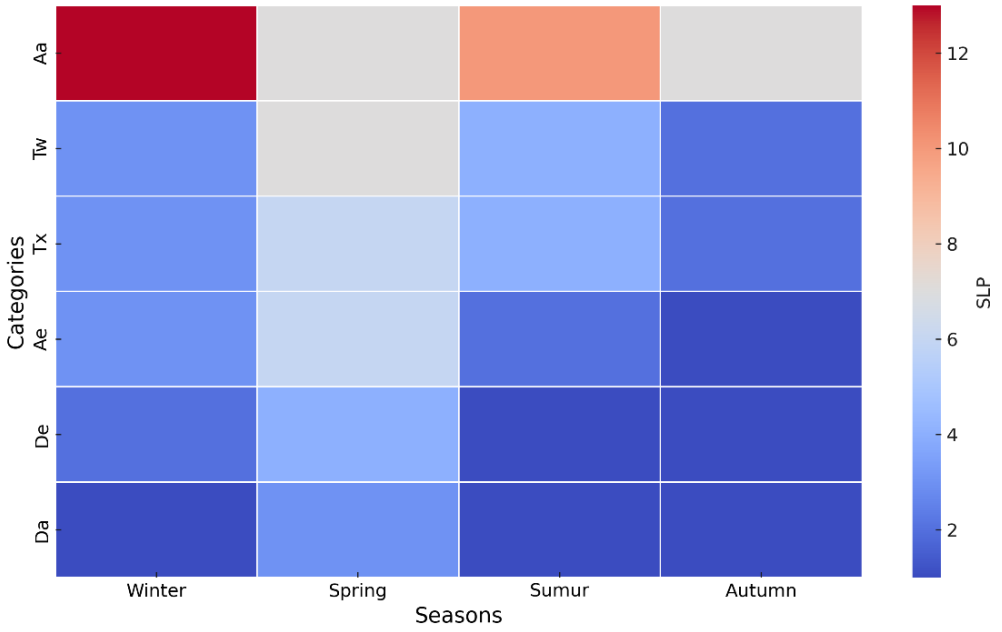

Figure 11. Seasonal distribution of sea-level pressure (SLP) configurations for Cloudy weather occurring at the margins of the frontal systems (3) conditions.
Source: Visualization created by the author based on categorized meteorological data (Chefchaouen Station).

The atmospheric dynamics at the 500 hPa level, depicted in Figure 12, demonstrate notable seasonal variations. The "Ng" structure, representing northern currents, is particularly active in both spring and summer, with 11 and 10 occurrences, respectively. This dominance of northern flows indicates a significant influence of cooler, stable air masses, which can suppress local instability but contribute to cloud formation without precipitation. Such northern currents are known to introduce stable, cold air that suppresses convective activity, leading to cloud formation under stable atmospheric conditions (Kim & Seo, 2023; Spiridonov & Ćurić, 2021). This behavior aligns with the general understanding of northern air masses at mid-level altitudes, where their interaction with warmer surface layers tends to stabilize the atmosphere, preventing major convective developments (Kim et al., 2023).

The atmospheric dynamics at the 500 hPa level, depicted in Figure 12, demonstrate notable seasonal variations. The "Sg" structure dominates during spring and summer, registering 11 and 10 occurrences, respectively, indicating stronger southern flows and an increase in cloud cover and instability. Additionally, the "Rc" structure is particularly active in spring, with 7 occurrences, reflecting the influence of weak ridge formations. During this phase, Chefchaouen lies on the southern margin of the northern jet stream, which predominantly flows over Europe. This positioning allows the jet stream to influence the region indirectly, with increased wind variability and cloud formation due to the interaction between the jet stream's upper-level dynamics and the weak southern ridges. While the jet stream helps contain the movement of these ridges, it also enhances local weather variability, contributing to cloud cover without precipitation. In contrast, the "Rd" structure is most prominent in summer, with 7 occurrences, suggesting increased upper-level divergence and a likely contribution to instability. Structures such as "Vc" and "Ve" show moderate activity, which has begun to increase in frequency compared to previous weather patterns. This shift suggests a complete change in the dynamics producing this weather pattern, compared to earlier ones, primarily in winter and spring, contributing to the seasonal variability in the weather patterns associated with frontal systems.

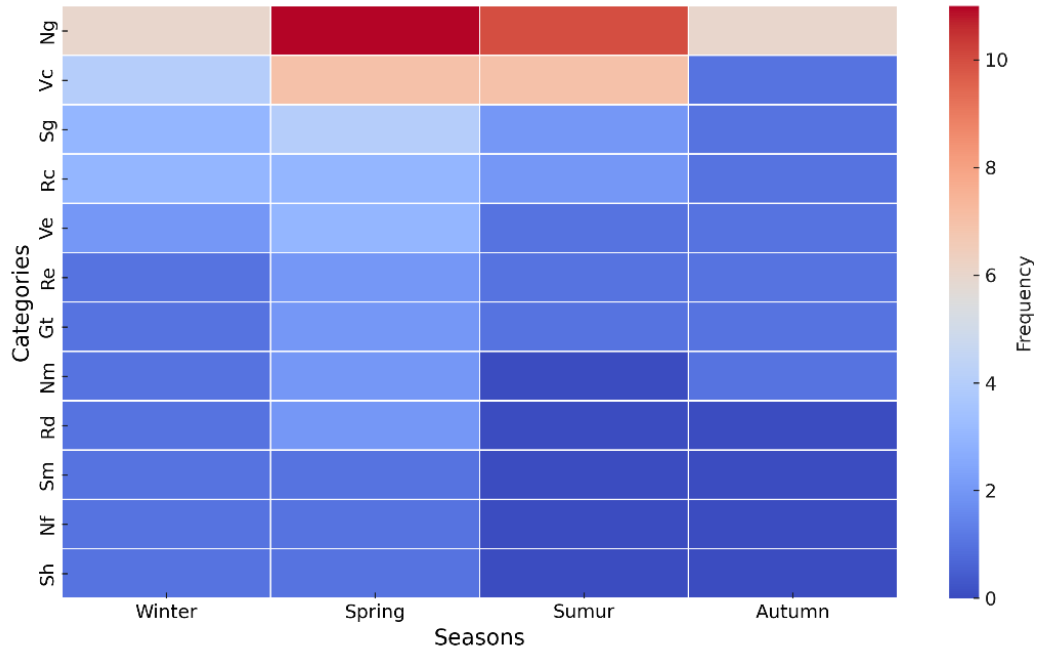

Figure 12. Seasonal distribution of sea-level pressure (500 hPa) configurations for Cloudy weather occurring at the margins of the frontal systems (3) conditions.
Source: Visualization created by the author based on categorized meteorological data (Chefchaouen Station).

These atmospheric configurations not only dictate the specific weather conditions prevalent during each season but also play a significant role in shaping the temperature dynamics associated with the 'Cloudy weather occurring at the margins of frontal systems (3)' pattern. The temperature gradient observed in this weather scenario diverges from previous patterns, as highlighted by a distinctive trend line depicted in violet. This trend shows a rapid decline from temperatures exceeding 30°C to below 8°C, particularly evident between structures (Cc-Im) and (Ve-Da). This pattern is visually illustrated in Figure 13.

The classification of cases with temperatures between 30.8°C and 21.6°C occurs at a rate of 33.6% of the total cases, indicating a relatively low frequency compared to other weather situation (Figure 13). Examining the controlling atmospheric patterns, we observe various branches of the ridge (Rc, Rb, Rd), followed by the southern current (Sg). Regarding mean sea level pressure (MSLP), transitional situations, particularly Situations (Tw) and (Tz), are most dominant and fluctuating.

In contrast, the classification of cases with temperatures between 15°C and 12°C constitutes 13% of the represented cases. At the GPH 500 hPa level, the northern current frequency (Ng) is noticeable, followed by valley forms (Vc, Ve), which significantly control the dynamics in this classification. These forms correspond, at the surface level, with the frequency of situations (Aa and Ae).

The weather system begins to change as the formations producing this type of weather condition shift compared to previous cases. The frequency of valleys fluctuates more, and a similar trend is observed with northern currents (Figure 13). The frequency of valleys (Vc) at the 500 hPa level indicates that polar influences start to prevail, suggesting a decline in hot subtropical influences towards the south. The sky transitions from clear or scattered clouds to being almost completely covered, with increasing wind strength, often from the west or northwest (Loikith et al., 2019; W. Zhang & Villarini, 2019).

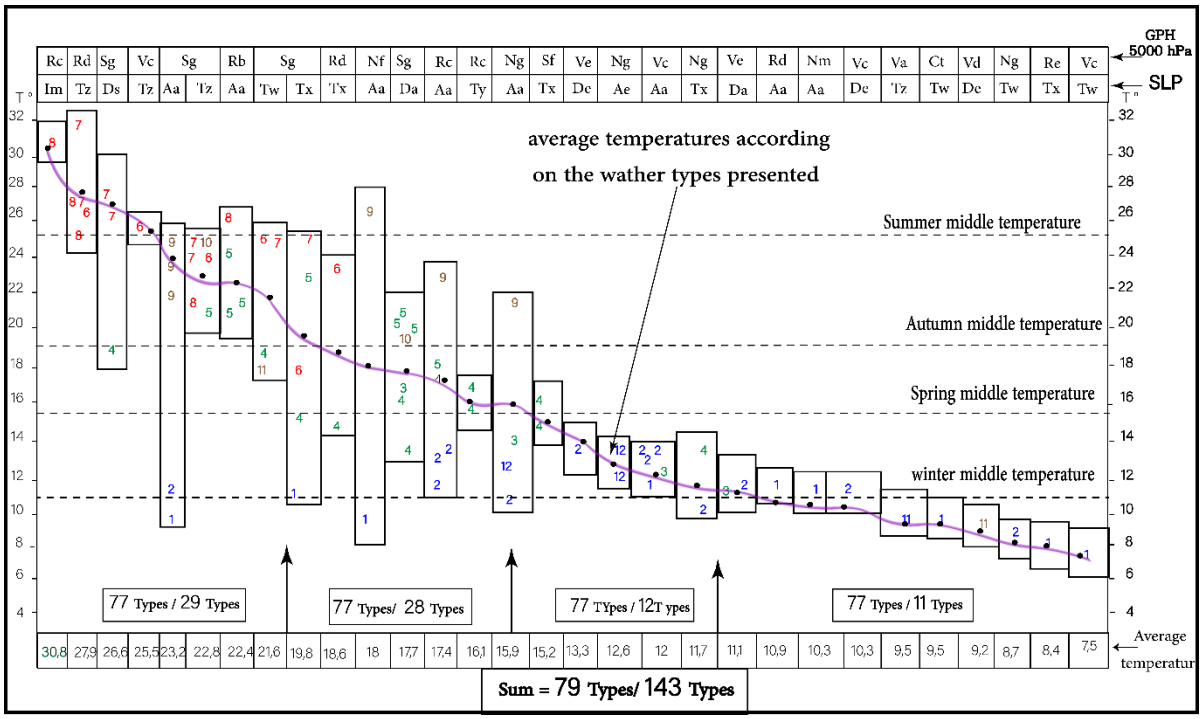

Figure 13. Impact of cloudy weather occurring at the margins of frontal systems on average temperatures at Chefchaouen Station, based on the analysis of atmospheric conditions at 500 hPa and sea level. This figure encompasses over 55% of the weather cases classified as type (3-1). A marked drop in average temperatures is observed, with the highest value reaching 30.8 °C under the (Cc-Im) configuration, and the lowest dropping to 7.5 °C under the (Vc-Tw) structure. This type of weather pattern often reflects a transition from stable to unstable atmospheric conditions, as illustrated by the frequent presence of valleys (Vc, Ve, Vd), southern flows (Sg, Sf), and northern flows (Ng, Nf, Nm) at 500 hPa. At sea level, these cases are commonly associated with low-pressure systems (Ds, De, Da) and transitional patterns (Tz, Tx, Ty), highlighting the dynamic nature of frontal margins in shaping thermal variability. Source: Created by the author based on processed meteorological data.

The classification of weather cases within the temperature range of 20°C to 16°C encompasses approximately 36.3% of the total cases, indicating a frequency close to previous classifications (Figure 13). This range is predominantly influenced by the southern current (S), particularly the movement (Sg), followed by the Ridge (Cc) with eight cases, and then the northern currents (Nf and Ng). These patterns correspond with the frequency of transitional situations (Tx and Tz) at MSLP, as well as a weak frequency of high-pressure systems concentrated over Europe (Ae) and the Atlantic Ocean (Aa).

In the temperature range of 12°C to 7.5°C, which accounts for 14.3% of the cases, most instances exhibit temperatures lower than the average winter temperature of 11°C (Figure 13). The valley forms, particularly (Vc), (Va), and (Vd), significantly contribute to this specific weather state. At the surface level, transitional (T) situations dominate with their various branches. Observations indicate a weak frequency of the Azores high-pressure (Aa) in this classification (Figure 23), primarily due to its southward shift attributed to polar descent. This shift opens the Atlantic gate for polar influences, especially during winter. This aligns with findings from studies on the North Atlantic subtropical anticyclone, documenting changes in the spatial and temporal patterns of the Azores high over the past century. The decline of high pressure in this region, especially during winter, suggests increased meridional flow and a greater prevalence of blocking anticyclones over Europe. Such dynamics have been linked to changes in greenhouse gas concentrations and their impact on atmospheric circulation patterns (Cresswell-Clay et al., 2022; Davis et al., 1997; Sinclair et al., 2020).

5. DISCUSSION

This study investigates the impact of cloudy weather patterns on daily temperature variations in Chefchaouen, located in the Western Rif Mountains of Morocco. By classifying non-rainy weather conditions and analyzing their influence on temperature dynamics, this research provides insights into the

role of atmospheric structures in regulating surface temperatures. The analysis identifies three primary categories of cloudy weather: cloudy weather with fairly stable atmospheric conditions (1), cloudy weather with quite unstable atmospheric conditions (2), and cloudy weather occurring at the margins of frontal systems (3). These categories exhibit distinct seasonal variations in temperature responses (see Table 2).

The findings reveal that during winter, category (1) corresponds to an average temperature of 10.6°C, whereas category (2) records 11.6°C, and category (3) exhibits 11.3°C. In contrast, during summer, temperatures rise to 25.4°C, 22.6°C, and 24.8°C for categories (1), (2), and (3), respectively. These variations indicate that cloudy weather with stable atmospheric conditions (1) contributes to greater thermal stability compared to unstable conditions (2), which exhibit more pronounced fluctuations due to atmospheric disturbances.

The observed thermal patterns align with previous findings by Dai et al., (1999), which highlight the dual role of cloud cover in reducing daytime solar radiation while enhancing nighttime heat retention. Furthermore, the presence of high-pressure systems at sea level and specific 500 hPa configurations explains the relatively stable temperature conditions observed during non-rainy periods. These results underscore the importance of synoptic-scale atmospheric structures in modulating local temperature variability.

Table 2. Average seasonal temperatures according to non-rainy weather patterns in Chefchaouen over the period 2015–2020.

weather type	winter C°	spring C°	summer C°	autumn C°
(1)	10,6	15,9	25,4	19,3
(2)	11,6	14,1	22,6	23,7
(3)	11,3	16,3	24,8	19,6

Source: Compiled by the author from classified temperature records at Chefchaouen Station.

This study further demonstrates the influence of cloudy weather patterns on seasonal and diurnal temperature regulation in Chefchaouen. The (2) weather pattern, characterized by unstable atmospheric conditions, results in lower summer temperatures (22.6°C) compared to both stable cloud cover (25.4°C). This cooling effect is particularly pronounced in spring and summer, consistent with findings by Groisman et al., (2000), who showed that dense cloud cover reduces surface solar radiation while increasing surface moisture, leading to overall lower temperatures. Similarly, Pyrgou et al., (2019) demonstrated that cloud cover plays a critical role in minimizing diurnal temperature range (DTR), especially during warm periods, by mitigating excessive daytime heating while preserving nighttime warmth.

These findings align with regional studies highlighting the stabilizing influence of cloud cover on temperature fluctuations. For instance, Xu et al., (2021)found that increased cloud cover in the Himalayas significantly reduces DTR across all seasons, with the strongest effects observed in winter. In Chefchaouen, the (2) and (3) cloud patterns moderate winter temperatures (11–12°C), contrasting with the lower values recorded under clear sky conditions. During summer, the presence of unstable (2) cloud cover results in lower overall temperatures (22.6°C) compared to the significantly higher temperatures observed under clear skies. These findings underscore the essential role of cloud cover in modulating seasonal temperature extremes.

Comparative analyses from European cities such as Athens and Madrid reinforce these conclusions, demonstrating that cloud cover strongly influences DTR during both heatwaves and typical summer days. The reduction in DTR under cloudy conditions in Chefchaouen, particularly during summer and spring, is consistent with results reported for other Mediterranean and mountainous climates (Hamal et al., 2021; Katavoutas et al., 2023; Pyrgou et al., 2019). While these findings corroborate existing research on the temperature-moderating effects of cloud cover, this study expands on previous work by focusing specifically on non-rainy weather patterns in a Mediterranean mountainous environment. This focus allows for a more refined understanding of how specific cloud types influence temperature fluctuations under dry atmospheric conditions.

The results also align with broader research on atmospheric circulation patterns and their influence on local climate dynamics. Studies by Loikith & Broccoli (2012) have demonstrated the relationship between positive geopotential height (GPH) anomalies at 500 hPa and sea-level pressure anomalies, showing their influence on regional temperature variations. Additionally, Connolly et al., (2021) and Yu & Lupo, (2019) highlight the impact of large-scale atmospheric systems on local thermal patterns. However, this study provides a novel contribution by isolating non-rainy atmospheric scenarios, thus refining our understanding of the specific mechanisms regulating temperature variations in Chefchaouen. By distinguishing different non-rainy cloud types, the study advances knowledge on local climate interactions and the thermal impacts of synoptic-scale atmospheric structures.

Despite offering valuable insights into the role of cloud cover in temperature regulation, some limitations should be acknowledged. First, the study is based exclusively on daily temperature data, which may not fully capture short-term fluctuations or transient atmospheric phenomena that influence local climate variability. Future research could incorporate higher-resolution temporal datasets to assess sub-daily temperature variations and detect rapid meteorological transitions. Second, the geographical focus on Chefchaouen limits the generalizability of these findings to regions with distinct topographical and climatic characteristics. Expanding the study to include a broader range of Mediterranean and mountainous locations could enhance the applicability of these results to diverse climate settings. Nonetheless, the robustness of the dataset, combined with detailed weather maps and local climatic analyses, provides a solid empirical foundation for the study's conclusions.

The implications of these findings are significant for practical applications, particularly in understanding the effects of cloudy weather on temperature. This can inform local climate adaptation strategies, urban planning, and natural resource management. For example, recognizing the temperature-modulating effects of cloud cover can guide the design of green spaces and urban layouts to mitigate heat stress (Meng et al., 2022). Additionally, these findings could contribute to the development of more accurate weather forecasting models that account for the specific impacts of cloudy conditions.

Beyond the theoretical contributions, these findings offer several practical implications that can inform decision-making processes in climate-sensitive sectors. The results of this study have practical applications for improving short- and medium-term weather forecasting in mountainous regions, particularly in predicting temperature variations under cloudy weather conditions. Moreover, understanding the influence of stable and unstable cloud conditions on local temperatures could guide the development of climate adaptation strategies for sectors such as agriculture and tourism in regions like the Western Rif. These strategies may include optimized scheduling for planting seasons, improved water resource management, and enhanced planning for tourism activities that are highly dependent on weather conditions.

Future studies should expand this research to include other regions and climatic conditions to verify the generalizability of the results. Furthermore, incorporating higher temporal resolution data and advanced modeling techniques could improve our understanding of short-term weather dynamics.

In summary, this study provides a comprehensive analysis of how cloudy weather types influence temperature patterns in Chefchaouen. The findings contribute to a deeper understanding of local atmospheric and climatic interactions, supporting efforts to improve local climate resilience and sustainable development planning. By highlighting the specific effects of different cloudy weather types, this research offers valuable insights into the broader field of climate and environmental management.

6. CONCLUSIONS

This study has provided a detailed examination of the influence of non-rainy weather patterns on temperature variations in Chefchaouen, located in the Western Rif Mountains of Morocco. By systematically classifying and analyzing daily temperature data in conjunction with atmospheric conditions at both sea level and the 500 hPa altitude, we were able to uncover the significant role these weather patterns play in shaping local temperature regimes.

Our analysis revealed that clear skies were the most dominant non-rainy weather type, representing 27% of all recorded cases. This weather type exhibited substantial temperature variation, especially in

summer, where high temperatures were closely associated with anticyclonic systems. Similarly, cloudy weather with fairly stable atmospheric conditions (classification 1), which accounted for 17.5% of the cases, demonstrated a strong link to ridges and barometric depressions, impacting both daytime and nighttime temperatures.

Additionally, cloudy weather with quite unstable atmospheric conditions (classification 2), which represented 16% of the cases, exhibited distinct thermal characteristics, particularly during transitional seasons. The least frequent weather type, cloudy weather occurring at the margins of frontal systems (classification 3), constituted 6.5% of the cases and was characterized by unique temperature gradients influenced by the interplay of polar and subtropical atmospheric systems.

These findings underscore the complexity of local climatic dynamics and emphasize the importance of integrating atmospheric parameters across multiple altitudes to fully understand temperature patterns. The insights gained from this study not only contribute to a more nuanced understanding of non-rainy weather influences but also offer valuable implications for refining regional climate models and enhancing local climate adaptation strategies in response to global climate change.

For future research, incorporating higher temporal resolution data would allow for a more detailed capture of short-term atmospheric events that were beyond the scope of this study. Additionally, extending this analysis to other geographically and climatically similar regions would further validate these findings and broaden their applicability. This research provides a vital foundation for both advancing scientific understanding of atmospheric dynamics and informing practical climate resilience measures.

Use of AI tools declaration

The author acknowledges that he has used AI-assisted tools, specifically ChatGPT, to assist in the organization, refinement, and editing of the manuscript. However, all intellectual contributions, analyses, and interpretations are the sole work of the author, ensuring the scientific integrity and originality of the research.

Author contributions

This work was conducted solely by the author, who has read and approved the final manuscript.

Conflicts of interest

The author declares no potential conflicts of interest with respect to the research, authorship, and/or publication of this article.

REFERENCES

Akinsanola, A. A., & Zhou, W. (2020). Understanding the Variability of West African Summer Monsoon Rainfall: Contrasting Tropospheric Features and Monsoon Index. *Atmosphere*, *11*(3), 309. https://doi.org/10.3390/atmos11030309

Beckert, A. A., Eisenstein, L., Oertel, A., Hewson, T., Craig, G. C., & Rautenhaus, M. (2023). The three-dimensional structure of fronts in mid-latitude weather systems in numerical weather prediction models. *Geoscientific Model Development*, *16*(15), 4427–4450. https://doi.org/10.5194/gmd-16-4427-2023

Bonino, G., Di Lorenzo, E., Masina, S., & Iovino, D. (2019). Interannual to decadal variability within and across the major Eastern Boundary Upwelling Systems. *Scientific Reports*, *9*(1), 19949. https://doi.org/10.1038/s41598-019-56514-8

Browning, K. A., Collier, C. G., Larke, P. R., Menmuir, P., Monk, G. A., & Owens, R. G. (1982). On the Forecasting of Frontal Rain Using a Weather Radar Network. *Monthly Weather Review*, *110*(6), 534–552. https://doi.org/10.1175/1520-0493(1982)110<0534:OTFOFR>2.0.CO;2

Byrne, M. P., & Schneider, T. (2018). Atmospheric Dynamics Feedback: Concept, Simulations, and Climate Implications. *Journal of Climate*, *31*(8), 3249–3264. https://doi.org/10.1175/JCLI-D-17-0470.1

Camici, S., Ciabatta, L., Massari, C., & Brocca, L. (2018). How reliable are satellite precipitation estimates for driving hydrological models: A verification study over the Mediterranean area. *Journal of Hydrology*, *563*, 950–961. https://doi.org/10.1016/j.jhydrol.2018.06.067

Connolly, M., Connolly, R., Soon, W., Velasco Herrera, V. M., Cionco, R. G., & Quaranta, N. E. (2021). Analyzing Atmospheric Circulation Patterns Using Mass Fluxes Calculated from Weather Balloon Measurements: North Atlantic Region as a Case Study. *Atmosphere*, *12*(11), 1439. https://doi.org/10.3390/atmos12111439

Cresswell-Clay, N., Ummenhofer, C. C., Thatcher, D. L., Wanamaker, A. D., Denniston, R. F., Asmerom, Y., & Polyak, V. J. (2022). Twentieth-century Azores High expansion unprecedented in the past 1,200 years. *Nature Geoscience*, *15*(7), 548–553. https://doi.org/10.1038/s41561-022-00971-w

Dai, A., Trenberth, K. E., & Karl, T. R. (1999). Effects of Clouds, Soil Moisture, Precipitation, and Water Vapor on Diurnal Temperature Range. *Journal of Climate*, *12*(8), 2451–2473. https://doi.org/10.1175/1520-0442(1999)012<2451:EOCSMP>2.0.CO;2

Davis, R. E., Hayden, B. P., Gay, D. A., Phillips, W. L., & Jones, G. V. (1997). The North Atlantic Subtropical Anticyclone. *Journal of Climate*, *10*(4), 728–744. https://doi.org/10.1175/1520-0442(1997)010<0728:TNASA>2.0.CO;2

Dezfuli, A. K., Zaitchik, B. F., & Gnanadesikan, A. (2015). Regional Atmospheric Circulation and Rainfall Variability in South Equatorial Africa. *Journal of Climate*, *28*(2), 809–818. https://doi.org/10.1175/JCLI-D-14-00333.1

Dilling, L., Pizzi, E., Berggren, J., Ravikumar, A., & Andersson, K. (2017). Drivers of adaptation: Responses to weather- and climate-related hazards in 60 local governments in the Intermountain Western U.S. *Environment and Planning A: Economy and Space*, *49*(11), 2628–2648. https://doi.org/10.1177/0308518X16688686

Doan, Q., Chen, F., Asano, Y., Gu, Y., Nishi, A., Kusaka, H., & Niyogi, D. (2022). Causes for Asymmetric Warming of Sub-Diurnal Temperature Responding to Global Warming. *Geophysical Research Letters*, *49*(20). https://doi.org/10.1029/2022GL100029

El Alaoui El Fels, A., Saidi, M. E., & Alam, M. J. Bin. (2022). Rainfall Frequency Analysis Using Assessed and Corrected Satellite Precipitation Products in Moroccan Arid Areas. The Case of Tensift Watershed. *Earth Systems and Environment*, *6*(2), 391–404. https://doi.org/10.1007/s41748-021-00290-x

El Baye A. (1990). *Recherches sur l'ambiance climatique dans le couloir d'Oujda-Taourirt (Maroc).* Université de Toulouse-la Mirail.

El Baye A. (1992). De la circulation aux temps: l'exemple des très beaux temps dans le nord-est du Maroc. *Publications de l'Association Intenationale de Climatologie*, *v*, 221–224.

El Kharim, Y., Bounab, A., Ilias, O., Hilali, F., & Ahniche, M. (2021). Landslides in the urban and suburban perimeter of Chefchaouen (Rif, Northern Morocco): inventory and case study. *Natural Hazards*, *107*(1), 355–373. https://doi.org/10.1007/s11069-021-04586-z

Fang, K., Gou, X., Chen, F., Li, J., D'Arrigo, R., Cook, E., Yang, T., & Davi, N. (2010). Reconstructed droughts for the southeastern Tibetan Plateau over the past 568 years and its linkages to the Pacific and Atlantic Ocean climate variability. *Climate Dynamics*, *35*(4), 577–585. https://doi.org/10.1007/s00382-009-0636-2

Fowler, H. J., Blenkinsop, S., & Tebaldi, C. (2007). Linking climate change modelling to impacts studies: recent advances in downscaling techniques for hydrological modelling. *International Journal of Climatology*, *27*(12), 1547–1578. https://doi.org/10.1002/joc.1556

García-Valero, J. A., Montavez, J. P., Jerez, S., Gómez-Navarro, J. J., Lorente-Plazas, R., & Jiménez-Guerrero, P. (2012). A seasonal study of the atmospheric dynamics over the Iberian Peninsula based on circulation types. *Theoretical and Applied Climatology*, *110*(1–2), 291–310. https://doi.org/10.1007/s00704-012-0623-0

Gatzen, C. P., Fink, A. H., Schultz, D. M., & Pinto, J. G. (2020). An 18-year climatology of derechos in Germany. *Natural Hazards and Earth System Sciences*, 1335–1351.

Ghassabi, Z., Fattahi, E., & Habibi, M. (2022). Daily Atmospheric Circulation Patterns and Their Influence on Dry/Wet Events in Iran. *Atmosphere*, *13*(1), 81. https://doi.org/10.3390/atmos13010081

Gillett, N. P., Kell, T. D., & Jones, P. D. (2006). Regional climate impacts of the Southern Annular Mode. *Geophysical Research Letters*, *33*(23). https://doi.org/10.1029/2006GL027721

Gonçalves, A. C. R., Nieto, R., & Liberato, M. L. R. (2023). Synoptic and Dynamical Characteristics of High-Impact Storms Affecting the Iberian Peninsula during the 2018–2021 Extended Winters. *Atmosphere*, *14*(9). https://doi.org/10.3390/atmos14091353

Grimm, A. M., Barros, V. R., & Doyle, M. E. (2000). Climate Variability in Southern South America Associated with El Niño and La Niña Events. *Journal of Climate*, *13*(1), 35–58. https://doi.org/10.1175/1520-0442(2000)013<0035:CVISSA>2.0.CO;2

Groisman, P. Y., Bradley, R. S., & Sun, B. (2000). The Relationship of Cloud Cover to Near-Surface Temperature and Humidity: Comparison of GCM Simulations with Empirical Data. *Journal of Climate*, *13*(11), 1858–1878. https://doi.org/10.1175/1520-0442(2000)013<1858:TROCCT>2.0.CO;2

Groisman, P. Y., Knight, R. W., Easterling, D. R., Karl, T. R., Hegerl, G. C., & Razuvaev, V. N. (2005). Trends in Intense Precipitation in the Climate Record. *Journal of Climate*, *18*(9), 1326–1350. https://doi.org/10.1175/JCLI3339.1

Hamal, K., Sharma, S., Talchabhadel, R., Ali, M., Dhital, Y. P., Xu, T., & Dawadi, B. (2021). Trends in the Diurnal Temperature Range over the Southern Slope of Central Himalaya: Retrospective and Prospective Evaluation. *Atmosphere*, *12*(12), 1683. https://doi.org/10.3390/atmos12121683

Horton, D. E., Johnson, N. C., Singh, D., Swain, D. L., Rajaratnam, B., & Diffenbaugh, N. S. (2015). Contribution of changes in atmospheric circulation patterns to extreme temperature trends. *Nature*, *522*(7557), 465–469. https://doi.org/10.1038/nature14550

Hoskins, B. J., & Karoly, D. J. (1981). The Steady Linear Response of a Spherical Atmosphere to Thermal and Orographic Forcing. *Journal of the Atmospheric Sciences*, *38*(6), 1179–1196. https://doi.org/10.1175/1520-0469(1981)038<1179:TSLROA>2.0.CO;2

Hufty, A. (2005). Situations synoptiques et analyse multivariée des temps à Québec. *Cahiers de Géographie Du Québec*, *20*(49), 69–92. https://doi.org/10.7202/021310ar

Jabbar, M. A. R., & Hassan, A. S. (2023). *The connection between 500 hPa geopotential height and heavy rainfall over Iraq: A case study*. 050002. https://doi.org/10.1063/5.0156846

James, P. M. (2007). An objective classification method for Hess and Brezowsky Grosswetterlagen over Europe. *Theoretical and Applied Climatology*, *88*(1–2), 17–42. https://doi.org/10.1007/s00704-006-0239-3

Jiang, S., Zhao, C., & Xia, Y. (2022). Distinct response of near surface air temperature to clouds in North China. *Atmospheric Science Letters*, *23*(12). https://doi.org/10.1002/asl.1128

Jones, P. D., Hulme, M., & Briffa, K. R. (1993). A comparison of Lamb circulation types with an objective classification scheme. *International Journal of Climatology*, *13*(6), 655–663. https://doi.org/10.1002/joc.3370130606

Kalisch, J., & Macke, A. (2008). Estimation of the total cloud cover with high temporal resolution and parametrization of short-term fluctuations of sea surface insolation. *Meteorologische Zeitschrift*, *17*(5), 603–611. https://doi.org/10.1127/0941-2948/2008/0321

Katavoutas, G., Founda, D., Varotsos, K. V., & Giannakopoulos, C. (2023). Diurnal Temperature Range and Its Response to Heat Waves in 16 European Cities—Current and Future Trends. *Sustainability*, *15*(17), 12715. https://doi.org/10.3390/su151712715

Kautz, L.-A., Martius, O., Pfahl, S., Pinto, J. G., Ramos, A. M., Sousa, P. M., & Woollings, T. (2022). Atmospheric blocking and weather extremes over the Euro-Atlantic sector – a review. *Weather and Climate Dynamics*, *3*(1), 305–336. https://doi.org/10.5194/wcd-3-305-2022

Kay, J. E., L'Ecuyer, T., Chepfer, H., Loeb, N., Morrison, A., & Cesana, G. (2016). Recent Advances in Arctic Cloud and Climate Research. *Current Climate Change Reports*, *2*(4), 159–169. https://doi.org/10.1007/s40641-016-0051-9

Kim, J.-Y., & Seo, K.-H. (2023). Physical mechanisms for the dominant summertime high-latitude atmospheric teleconnection pattern and the related Northern Eurasian climates. *Environmental Research Letters*, *18*(10), 104022. https://doi.org/10.1088/1748-9326/acfa13

Kim, M. H., Lee, J., & Lee, S.-J. (2023). Hail: Mechanisms, Monitoring, Forecasting, Damages, Financial Compensation Systems, and Prevention. *Atmosphere*, *14*(11), 1642. https://doi.org/10.3390/atmos14111642

Kolendowicz, L., Półrolniczak, M., Kendzierski, S., Szyga-Pluta, K., & Láska, K. (2021). Influence of Atmospheric Circulation on Cloudiness and Cloud Types in Petuniabukta and Svalbard-Lufthavn in Summer 2016. *Atmosphere*, *12*(6), 724. https://doi.org/10.3390/atmos12060724

Lamb, H. H. (1972). British isles weather types and a register of the daily sequence of circu lation patterns 1861-1971. *Geophysical Memoirs*, *16*(116), 1–85.

Lennard, C., & Hegerl, G. (2015). Relating changes in synoptic circulation to the surface rainfall response using self-organising maps. *Climate Dynamics*, *44*(3–4), 861–879. https://doi.org/10.1007/s00382-014-2169-6

Li, W., Duan, L., Luo, Y., Liu, T., & Scharaw, B. (2018). Spatiotemporal Characteristics of Extreme Precipitation Regimes in the Eastern Inland River Basin of Inner Mongolian Plateau, China. *Water*, *10*(1), 35. https://doi.org/10.3390/w10010035

Lionello, P. , M.-R. P. , & B. R. (2006). *Mediterranean climate variability* (Elsevier).

Liu, C., Susilo, Y. O., & Karlström, A. (2014). Examining the impact of weather variability on non-commuters' daily activity–travel patterns in different regions of Sweden. *Journal of Transport Geography*, *39*, 36–48. https://doi.org/10.1016/j.jtrangeo.2014.06.019

Loikith, P. C., & Broccoli, A. J. (2012). Characteristics of Observed Atmospheric Circulation Patterns Associated with Temperature Extremes over North America. *Journal of Climate*, *25*(20), 7266–7281. https://doi.org/10.1175/JCLI-D-11-00709.1

Loikith, P. C., & Kalashnikov, D. A. (2023). Meteorological Analysis of the Pacific Northwest June 2021 Heatwave. *Monthly Weather Review*, *151*(5), 1303–1319. https://doi.org/10.1175/MWR-D-22-0284.1

Loikith, P. C., Pampuch, L. A., Slinskey, E., Detzer, J., Mechoso, C. R., & Barkhordarian, A. (2019). A climatology of daily synoptic circulation patterns and associated surface meteorology over southern South America. *Climate Dynamics*, *53*(7–8), 4019–4035. https://doi.org/10.1007/s00382-019-04768-3

Lu, X., Zhang, L., & Shen, L. (2019). Meteorology and Climate Influences on Tropospheric Ozone: a Review of Natural Sources, Chemistry, and Transport Patterns. *Current Pollution Reports*, *5*(4), 238–260. https://doi.org/10.1007/s40726-019-00118-3

Luo, H., Quaas, J., & Han, Y. (2024). Diurnally asymmetric cloud cover trends amplify greenhouse warming. *Science Advances*, *10*(25). https://doi.org/10.1126/sciadv.ado5179

Mashoudi, A. Al, Akallouch, A., Ziani, M., & Mousaoui, M. El. (2024). Exploring the impact of weather patterns on exceptional flooding events in the Nekor watershed, NE Morocco. *Environmental & Socio-Economic Studies*, *12*(1), 1–12. https://doi.org/10.2478/environ-2024-0001

Meng, A., Wen, D., & Zhang, C. (2022). Maize Seed Germination Under Low-Temperature Stress Impacts Seedling Growth Under Normal Temperature by Modulating Photosynthesis and Antioxidant Metabolism. *Frontiers in Plant Science*, *13*. https://doi.org/10.3389/fpls.2022.843033

Mills, L. , J. J. , & M. F. (2024). Baseline climatology of the Canary Current Upwelling System and evolution of sea surface temperature. *Remote Sensing*.

Mohamed Arraji. (1995). *Le climat du versant méditerranéen du Rif central (Maroc) : une géographie de la pluie, mécanismes pluviogènes et temps pluvieux*. Toulouse 2.

Mülmenstädt, J., Salzmann, M., Kay, J. E., Zelinka, M. D., Ma, P.-L., Nam, C., Kretzschmar, J., Hörnig, S., & Quaas, J. (2021). An underestimated negative cloud feedback from cloud lifetime changes. *Nature Climate Change*, *11*(6), 508–513. https://doi.org/10.1038/s41558-021-01038-1

Newton, B. W., Prowse, T. D., & Bonsal, B. R. (2014). Evaluating the distribution of water resources in western Canada using synoptic climatology and selected teleconnections. Part 1: winter season. *Hydrological Processes*, *28*(14), 4219–4234. https://doi.org/10.1002/hyp.10233

Peña, J. C., Aran, M., Cunillera, J., & Amaro, J. (2011). Atmospheric circulation patterns associated with strong wind events in Catalonia. *Natural Hazards and Earth System Sciences*, *11*(1), 145–155. https://doi.org/10.5194/nhess-11-145-2011

Pereira, S. C., Carvalho, D., & Rocha, A. (2021). Temperature and Precipitation Extremes over the Iberian Peninsula under Climate Change Scenarios: A Review. *Climate*, *9*(9), 139. https://doi.org/10.3390/cli9090139

Perkins, S. E., Alexander, L. V., & Nairn, J. R. (2012). Increasing frequency, intensity and duration of observed global heatwaves and warm spells. *Geophysical Research Letters*, *39*(20). https://doi.org/10.1029/2012GL053361

Philipp, A. (2009). Comparison of principal component and cluster analysis for classifying circulation pattern sequences for the European domain. *Theoretical and Applied Climatology*, *96*(1–2), 31–41. https://doi.org/10.1007/s00704-008-0037-1

Pyrgou, A., Santamouris, M., & Livada, I. (2019). Spatiotemporal Analysis of Diurnal Temperature Range: Effect of Urbanization, Cloud Cover, Solar Radiation, and Precipitation. *Climate*, *7*(7), 89. https://doi.org/10.3390/cli7070089

Raissouni, N., Sobrino, J. A., Chahboun, A., Ben Achhab, N., Lahraoua, M., & Azyat, A. (2013). First results towards building up a reliable *in situ* measurements database for LST algorithm validations using modular WSN: Northern Morocco campaigns case study. *International Journal of Remote Sensing*, *34*(9–10), 3153–3163. https://doi.org/10.1080/01431161.2012.716533

Rojas, M., Li, L. Z., Kanakidou, M., Hatzianastassiou, N., Seze, G., & Le Treut, H. (2013). Winter weather regimes over the Mediterranean region: their role for the regional climate and projected changes in the twenty-first century. *Climate Dynamics*, *41*(3–4), 551–571. https://doi.org/10.1007/s00382-013-1823-8

Semedo, A. (2018). Seasonal Variability of Wind Sea and Swell Waves Climate along the Canary Current: The Local Wind Effect. *Journal of Marine Science and Engineering*, *6*(1), 28. https://doi.org/10.3390/jmse6010028

Sinclair, V. A., Rantanen, M., Haapanala, P., Räisänen, J., & Järvinen, H. (2020). The characteristics and structure of extra-tropical cyclones in a warmer climate. *Weather and Climate Dynamics*, *1*(1), 1–25. https://doi.org/10.5194/wcd-1-1-2020

Spiridonov, V., & Ćurić, M. (2021). Cyclones and Anticyclones. In *Fundamentals of Meteorology* (pp. 263–273). Springer International Publishing. https://doi.org/10.1007/978-3-030-52655-9_17

Sun, B., Groisman, P. Y., Bradley, R. S., & Keimig, F. T. (2000). Temporal Changes in the Observed Relationship between Cloud Cover and Surface Air Temperature. *Journal of Climate*, *13*(24), 4341–4357. https://doi.org/10.1175/1520-0442(2000)013<4341:TCITOR>2.0.CO;2

Teng, H., & Branstator, G. (2017). Causes of Extreme Ridges That Induce California Droughts. *Journal of Climate*, *30*(4), 1477–1492. https://doi.org/10.1175/JCLI-D-16-0524.1

Trigo, I. F., & Viterbo, P. (2003). Clear-Sky Window Channel Radiances: A Comparison between Observations and the ECMWF Model. *Journal of Applied Meteorology*, *42*(10), 1463–1479. https://doi.org/10.1175/1520-0450(2003)042<1463:CWCRAC>2.0.CO;2

Vigneau JP. (1985). *Climat et climats des pyrénées Orientales*. Université de Dijon.

Wang, Y., Xu, M., Li, J., Jiang, N., Wang, D., Yao, L., & Xu, Y. (2020). The Gradient Effect on the Relationship between the Underlying Factor and Land Surface Temperature in Large Urbanized Region. *Land*, *10*(1), 20. https://doi.org/10.3390/land10010020

Xu, X., Lyu, D., Lei, X., Huang, T., Li, Y., Yi, H., Guo, J., He, L., He, J., Yang, X., Guo, M., Liu, B., & Zhang, X. (2021). Variability of extreme precipitation and rainfall erosivity and their attenuated effects on sediment delivery from 1957 to 2018 on the Chinese Loess Plateau. *Journal of Soils and Sediments*, *21*(12), 3933–3947. https://doi.org/10.1007/s11368-021-03054-2

Yang, Y., Liu, Y., Hu, Z., Yu, H., Li, J., Xie, Y., & Yang, Q. (2023). Impact of the leading atmospheric wave train over Eurasia on the climate variability over the Tibetan Plateau during early spring. *Climate Dynamics*, *60*(11–12), 3885–3900. https://doi.org/10.1007/s00382-022-06525-5

Yu, B., & Lupo, A. R. (2019). Large-Scale Atmospheric Circulation Variability and Its Climate Impacts. *Atmosphere*, *10*(6), 329. https://doi.org/10.3390/atmos10060329

Zappa, G. (2019). Regional Climate Impacts of Future Changes in the Mid–Latitude Atmospheric Circulation: a Storyline View. *Current Climate Change Reports*, *5*(4), 358–371. https://doi.org/10.1007/s40641-019-00146-7

Zhang, W., & Villarini, G. (2019). On the weather types that shape the precipitation patterns across the U.S. Midwest. *Climate Dynamics*, *53*(7–8), 4217–4232. https://doi.org/10.1007/s00382-019-04783-4

Zhang, X., Alexander, L., Hegerl, G. C., Jones, P., Tank, A. K., Peterson, T. C., Trewin, B., & Zwiers, F. W. (2011). Indices for monitoring changes in extremes based on daily temperature and precipitation data. *WIREs Climate Change*, *2*(6), 851–870. https://doi.org/10.1002/wcc.147

Zhu, X.-M., Song, X.-N., Li, X.-T., Zhou, F.-C., & Guo, H. (2024). A Physical Process-Based Enhanced Adjacent Channel Retrieval Algorithm for Obtaining Cloudy-Sky Surface Temperature. *IEEE Transactions on Geoscience and Remote Sensing*, *62*, 1–13. https://doi.org/10.1109/TGRS.2023.3344757

Appendix I. Cloudy Weather with Fairly Stable Atmospheric Conditions on October 1, 2019 (Sky Coverage 1/8)

This figure illustrates the weather condition of "Cloudy weather with fairly stable atmospheric conditions" observed on October 1, 2019, with approximately 1/8 cloud cover, measured in oktas. This sparse cloud coverage, shown in the satellite image, highlights limited cloud formation over northern Morocco, particularly in the areas surrounding Chefchaouen.

The synoptic chart reveals relatively stable atmospheric pressure with weak pressure gradients, conducive to minimal cloud development. The accompanying geopotential height map at 500 hPa further supports these observations, indicating a stable upper atmosphere with limited dynamic weather systems, which is consistent with the partly cloudy sky observed in the satellite image.

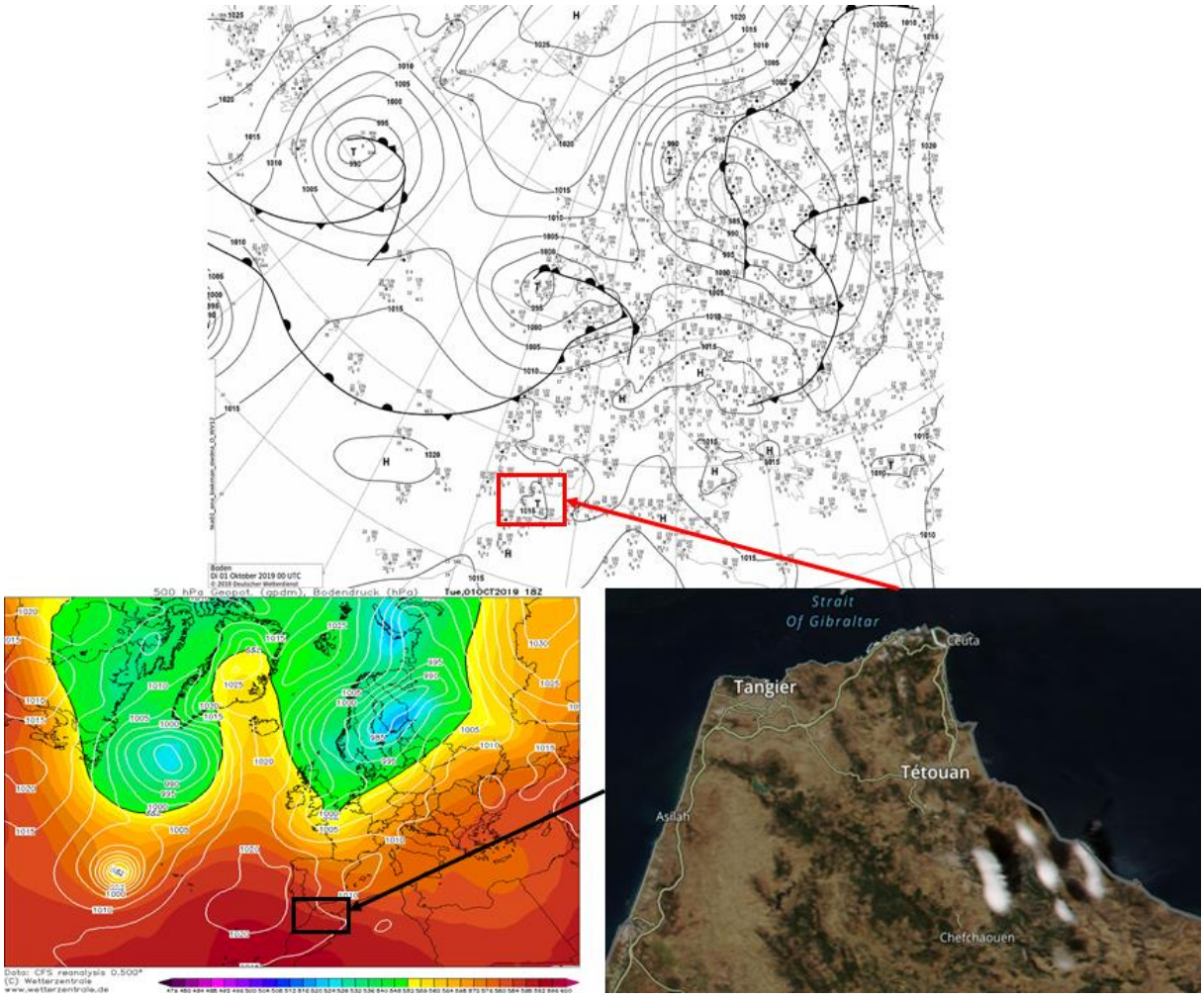

Appendix II. Cloudy Weather with Quite Unstable Atmospheric Conditions on June 13, 2019

This figure illustrates "Cloudy weather with quite unstable atmospheric conditions" observed on June 13, 2019, with approximately 4 oktas of sky coverage. The satellite image shows moderate cloud formation, particularly over northern Morocco, including Chefchaouen, suggesting a completely unstable atmosphere conducive to more dynamic weather changes.

The synoptic chart reveals tightly packed isobars, indicating stronger pressure gradients, which contribute to the marked instability in the atmosphere. The 500 hPa geopotential height map further highlights the presence of upper-level troughs and dynamic weather systems, reinforcing the unstable conditions that led to moderate cloud cover and rapid fluctuations in weather patterns, as depicted in the satellite image.

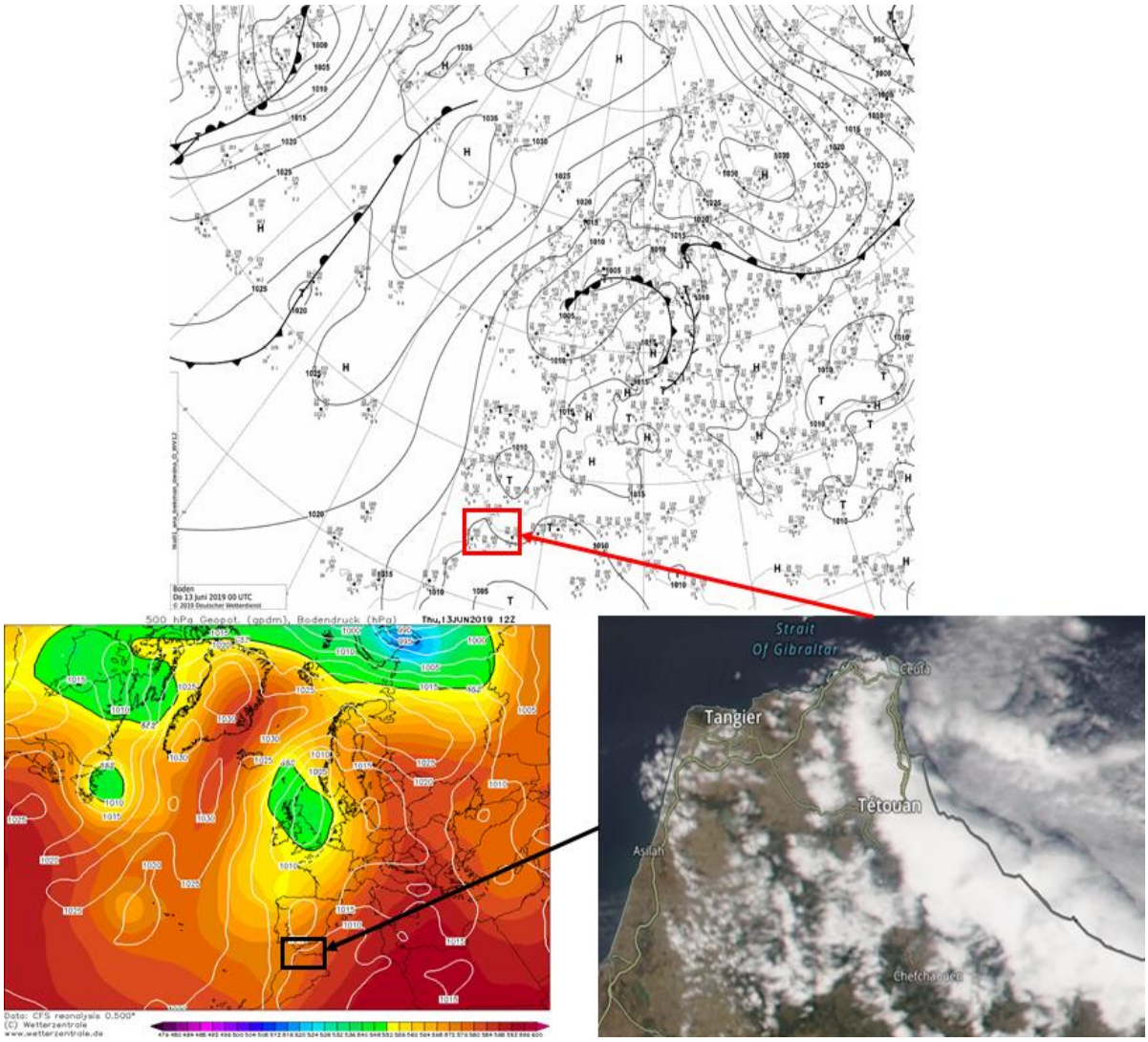

Appendix III. Cloudy Weather at the Margins of a Frontal System on November 8, 2018

The figure illustrates "Cloudy weather occurring at the margins of the frontal systems", observed on November 8, 2018. The satellite image reveals significant cloud cover over northern Morocco, particularly around Tangier, Tetouan, and Chefchaouen. These clouds, although widespread, are not associated with heavy precipitation, as they are located at the periphery of a nearby frontal system.

The synoptic chart highlights low-pressure systems near the region, as seen on November 8, 2018, which facilitates the formation of these clouds at the edges of the front. This type of weather is typical when the region experiences cloud covers due to adjacent pressure systems, resulting in overcast skies without intense weather phenomena.

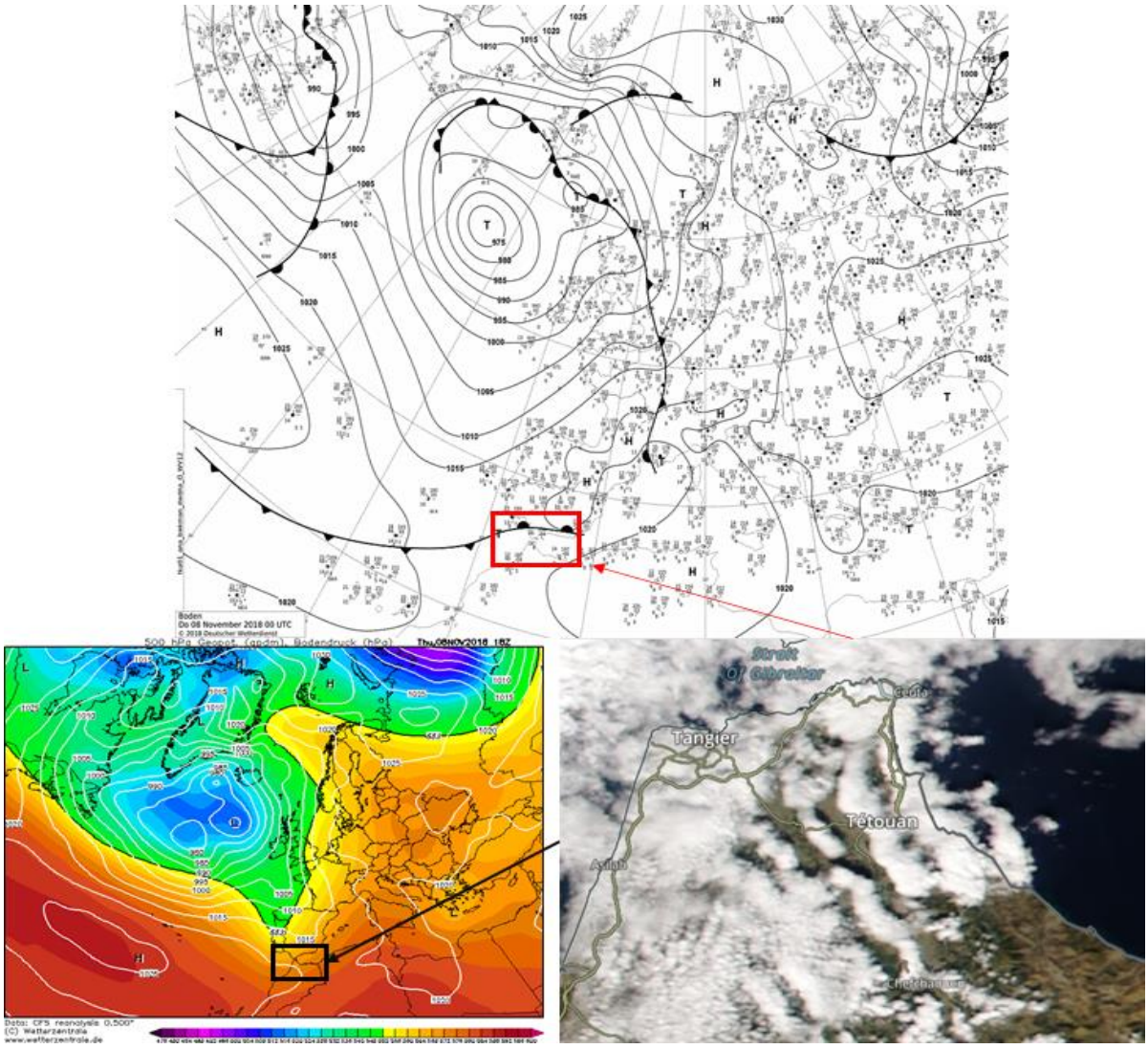

Appendix IV. Classification and Illustration of Atmospheric Circulation Patterns at GPH 500 hPa and Mean Sea Level Pressure (MSLP)

These figures provide a detailed representation of the significant atmospheric conditions observed over the past six years, derived from systematic daily analyses of synoptic weather patterns. The first figure illustrates the dominant circulation structures at the 500 hPa pressure level, highlighting the large-scale atmospheric dynamics that influence temperature variability in the Western Rif region. The colored lines correspond to distinct air mass movements and atmospheric configurations, each assigned a specific code to facilitate interpretation. These configurations reflect variations in pressure gradients, ridge-trough interactions, and the overall atmospheric stability that governs cloud cover formation and thermal fluctuations.

The second figure focuses on sea-level pressure (MSLP) variations, capturing key meteorological situations recorded between 2015 and 2020. This representation is crucial for understanding how surface-level high and low-pressure systems contribute to local climate dynamics. The patterns depicted in this figure emphasize the influence of synoptic-scale pressure anomalies, including the positioning of anticyclones, cyclonic depressions, and transition zones. These elements play a fundamental role in modulating temperature distributions, affecting the extent and persistence of non-precipitating cloud cover in the study area.

By integrating these atmospheric insights, these figures serve as essential references for interpreting the interaction between upper-atmosphere circulation (500 hPa) and surface pressure systems (MSLP), thereby enhancing our understanding of regional weather variability in Chefchaouen and the broader Western Rif region.

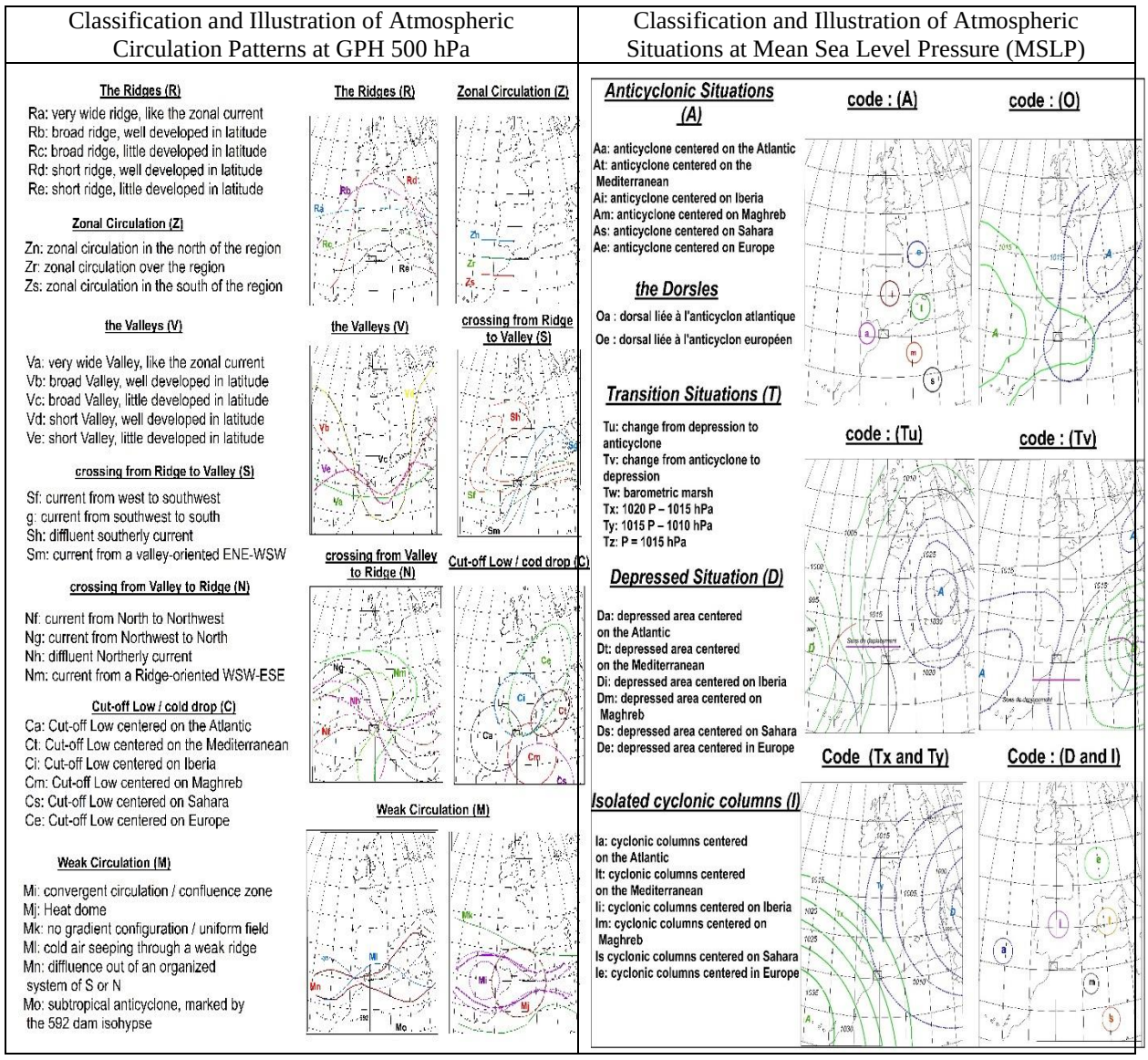

Source: Adapted and modified from Vigneau (1985), with updates by El Baye (1990) and further modifications by the author.